# Peripheral opioid receptor antagonism alleviates fentanyl-induced cardiorespiratory depression and is devoid of aversive effects

[1,2,3]Brian C. Ruyle, [1,2,3]Sarah Masud, [1,2,3]Rohith Kesaraju, [1,2,3]Mubariz Tahirkheli, [1,2,3]Juhi Modh, [1,2,3]Caroline Roth, [1,2,3]Sofia Angulo-Lopera, [1,2,3]Tania Lintz, [1,2,3]Jessica A. Higginbotham, [1,2,3]Nicolas Massaly, [1,2,3,4,5]Jose A Moron*

## Affiliations:

[1]Department of Anesthesiology, Washington University in St Louis; St. Louis, MO, USA

[2]Pain Center, Washington University in St Louis; St. Louis, MO, USA

[3]School of Medicine, Washington University in St. Louis; St. Louis, MO, USA

[4]Department of Neuroscience, Washington University in St. Louis; St. Louis, MO, USA

[5]Department of Psychiatry, Washington University in St. Louis; St. Louis, MO, USA

*corresponding author Email: jmoron-concepcion@wustl.edu

## ABSTRACT

Millions of Americans suffering from Opioid Use Disorders (OUD) face a high risk of fatal overdose due to opioid-induced respiratory depression (OIRD). Fentanyl, a powerful synthetic opioid, is a major contributor to the rising rates of overdose deaths. Reversing fentanyl-induced respiratory depression has proved to be challenging due to both its high potency and lipophilicity. We assessed the contributions of central and peripheral mu opioid receptors (MORs) in mediating fentanyl-induced physiological responses. The peripherally restricted MOR antagonist naloxone methiodide (NLXM) both prevented and reversed OIRD to a comparable degree as naloxone (NLX), indicating substantial involvement of peripheral MORs during OIRD. Interestingly, NLXM-mediated OIRD reversal did not produce aversive behaviors observed after NLX. We show that neurons in the nucleus of the solitary tract (nTS), the first central synapse of peripheral afferents, exhibit biphasic patterns of activity following fentanyl exposure. NLXM pretreatment attenuates this activity, suggesting that these responses are mediated by peripheral MORs. Together, these findings establish a critical role for peripheral MOR, including ascending inputs to the nTS, as sites of dysfunction during OIRD. Furthermore, selective peripheral MOR antagonism could be a promising therapeutic strategy for managing OIRD by sparing CNS-driven acute opioid-associated withdrawal and aversion observed after NLX.

## Keywords

Opioids, brainstem, respiratory depression, opioid receptors, fentanyl

## Significance Statement:

In this study, we compare the central versus peripheral components underlying fentanyl-induced cardiorespiratory depression to prevent overdose deaths. Our data indicate that these effects are, at least partially, due to the activation of mu opioid receptors present in peripheral sites. These findings provide insight into peripheral contributions to fentanyl-induced overdoses and could potentially lead to the development of treatments selectively targeting the peripheral system, sparing individuals from the CNS-driven acute opioid withdrawal generally observed with the use of naloxone.

## INTRODUCTION

Millions of Americans live with Opioid Use Disorders (OUD) and face a high risk of opioid-induced respiratory depression (OIRD), the leading cause of opioid related deaths (*1*). The number of fatalities attributed to OIRD has been exacerbated by the rise of distribution and use of synthetic opioids, such as fentanyl (*2–5*). Fentanyl is a highly lipophilic opioid that readily crosses the blood-brain barrier and binds tightly to mu opioid receptors (MORs), which are abundant in the respiratory centers of the brainstem (*1*, *6*, *7*). Compared to other opioids such as heroin and morphine, fentanyl exhibits both a faster onset of OIRD and higher potency for MOR binding (*8*, *9*), minimizing successful prevention of lethal outcomes using naloxone (NLX), a competitive and preferential MOR antagonist (*10*, *11*). Despite its high efficacy in reversing OIRD, NLX also precipitates unpleasant withdrawal symptoms and aversion, as reported in patients and preclinical models (*11–14*), making its implementation for managing OUD challenging. Therefore, a better understanding of the pharmacology, specific brain regions and pathways, and physiological responses induced by high doses of fentanyl are necessary to develop effective prevention and intervention strategies, ultimately saving lives of patients suffering from OUD.

Several regions have been implicated as key sites of triggering OIRD, including the Pre-Botzinger Complex in the ventral medulla and the parabrachial nucleus and Kolliker-Fuse nucleus in the pons (*1*, *15–20*). Opioids act directly within these networks to alter inspiratory and expiratory phase duration, leading to overall reductions in respiratory rate and apneas (*18*, *20*, *21*). In addition, the nucleus of the solitary tract (nTS), located in the dorsal brainstem, is the first central site that receives sensory afferent information via cranial nerves related to cardiorespiratory, gustatory and gastrointestinal function (*22*). Acute hypoxia robustly activates nTS neurons (*23*, *24*) to initiate appropriate autonomic and cardiorespiratory responses that

facilitate a return to homeostatic physiological states. MOR is highly expressed in the nTS, primarily on vagal afferent fibers that terminate within the nTS(*25*). Opioids induce both systemic and brain hypoxia (*26*, *27*) and produce an increase in Fos-immunoreactivity in the nTS (*28*, *29*). However, engaging MOR signaling in the nTS impairs hypoxic ventilatory responses (*7*). This suggests that OIRD may result from nTS dysfunction failing to engage appropriate cardiorespiratory responses, thereby leading to prolonged OIRD. However, the specific contributions of nTS MOR, including ascending MOR-expressing inputs from the periphery to this region, in driving aberrant cardiorespiratory depression are still not fully understood.

In addition to their high expression throughout brainstem respiratory nuclei, MORs are also expressed in the periphery, including sensory ganglia, lung afferents, cardiac tissue and cranial nerves that terminate within the nTS (*30*, *31*). Naloxone Methiodide (NLXM) is a quaternary derivative of NLX that does not cross the blood brain barrier at low doses, making it a useful tool to assess the peripheral vs central contribution of MORs in opioid-induced physiology and behavior (*10*, *32*). Despite its lower binding affinity for MOR(*10*), NLXM has been shown to reverse opioid-induced hypoventilation and brain hypoxia in rodent models (*12*, *32*, *33*), suggesting that peripheral opioid receptors may play a greater role in OIRD than previously thought. However, no studies to date have provided a comprehensive assessment of opioid-induced cardiorespiratory depression and systemic hypoxia combined with a real-time assessment of MOR-mediated activity of nTS neurons.

In the present study, we examined the relative contributions of central and peripheral MORs mediating fentanyl-induced depression of cardiorespiratory parameters and investigated potential mechanisms of opioid-induced dysfunction within the nTS. We report that fentanyl-induced cardiorespiratory depression and prolonged systemic hypoxia can be prevented or reversed by NLXM to a degree similar to NLX. As compared to NLX, NLXM-mediated reversal of OIRD did not produce aversive-like behaviors. Fentanyl induced robust Fos-IR expression in the nTS in a dose-dependent manner, and this activation can be attributed to a combination of direct effects of opioids acting at MOR located within the nTS and the subsequent hypoxia that develops after fentanyl exposure. Given that the majority of nTS MOR is located on vagal afferent fibers, we utilized various techniques to evaluate opioid-induced activity within the nTS and manipulate nTS MOR signaling during OIRD. Using wireless *in vivo* fiber photometry, we show that fentanyl induces a biphasic pattern of activity in nTS, characterized by a transient increase followed by a prolonged decrease in neuronal excitability. NLXM pretreatment strongly attenuated this biphasic response, indicating that fentanyl-induced nTS activity is influenced by

MOR-expressing peripheral afferents. Together, these findings provide novel insights into peripheral mechanisms mediating OIRD and support peripheral MOR antagonism as a promising therapeutic strategy for managing OIRD for patients suffering from OUD while sparing the CNS-driven acute aversive behaviors that are observed with the use of NLX.

# RESULTS

### Intravenous fentanyl induces respiratory depression and activates nTS neurons in a dose-dependent manner

We first examined the effect of intravenous fentanyl to induce cardiorespiratory depression and activate neurons in the nucleus tractus solitarius (nTS). Catheterized rats received intravenous saline (1 ml/kg) or fentanyl at a range of doses (2, 20, or 50 µg/kg; **Figure 1A**), and cardiorespiratory parameters were measured up to 60 minutes. The first 20 minutes of these responses are shown in **Figure 1B-D**. As shown in **Table 1**, baseline cardiorespiratory parameters were similar between male and female rats that received 20 µg/kg fentanyl. There was a small but significant difference in basal heart rate in female rats that received 50 µg/kg fentanyl (**Table 2**). Neither saline nor 2 µg/kg fentanyl evoked a significant change in cardiorespiratory parameters. In comparison, both 20 and 50 µg/kg fentanyl produced rapid decreases in oxygen saturation, heart rate, and respiratory rate, with the largest decrease occurring after 50 µg/kg fentanyl. The nadir (defined as the lowest point measured after fentanyl) and recovery (calculated as 90% of baseline values prior to fentanyl) for each physiological parameter were assessed in all groups (**Figure 1E-J**). There was no significant difference in the nadir or recovery values between saline- and 2 µg/kg fentanyl-treated rats. In comparison, rats given 50 µg/kg fentanyl exhibited a significantly lower nadir in oxygen saturation (**Figure 1E**) and respiratory rate (**Figure 1I**) compared to 20 µg/kg. In addition, the recovery time was significantly longer in rats that received 50 µg/kg fentanyl compared to 20 µg/kg fentanyl (**Figure 1F,J)**. The nadir of bradycardia was similar between 20- and 50 µg/kg rats (**Figure 1G**), although the duration of the response was significantly longer in rats that received the highest dose of fentanyl (**Figure 1H**). Overall, we observed no sex differences in the nadir or recovery time in rats that received 20 µg/kg fentanyl. Female rats that received 50 µg/kg fentanyl exhibited a significantly longer recovery of respiratory rate, although oxygen saturation and heart rate recover times were similar to males (**Table 3,4**). We next examined nTS activation (Fos-IR) following intravenous fentanyl (**Figure 1K)**. A significant increase in Fos-IR was observed after 2 µg/kg fentanyl, (**Figure 1L**), a dose that did not induce cardiorespiratory depression. Further dose-dependent increases in Fos-IR were observed after

20 and 50 µg/kg fentanyl. We evaluated a subpopulation of catecholaminergic nTS neurons, which are critical for full expression of hypoxia-evoked cardiorespiratory responses (*23*, *34*) for activation after intravenous fentanyl (**Figure 1M**). These cells were similarly activated at 2 and 20 µg/kg fentanyl, with a further increase observed at the highest dose (50 µg/kg).

**Peripheral opioid receptor antagonism prevents fentanyl-induced respiratory depression**

The above data provide a comprehensive assessment of the dose-dependent changes in cardiorespiratory parameters and nTS neuronal activation evoked by intravenous fentanyl. To gain insight into the extent to which central and peripheral opioid receptors mediate these effects, separate cohorts of rats received intravenous administration of the centrally and peripherally acting competitive opioid receptor antagonist naloxone (NLX; 1 mg/kg) or the peripherally restricted opioid receptor antagonist naloxone methiodide (NLXM, 1 and 5 mg/kg) prior to intravenous fentanyl administration at 20 µg/kg (**Figure 2A**) or 50 µg/kg (**Figure S1A**). It has been previously shown that NLXM does not cross the blood brain barrier at low doses (*32*, *35*). Our biodistribution data are in agreement with these reports. Catheterized rats that received intravenous NLXM (1 or 5 mg/kg) or NLX (1 mg/kg) were evaluated for detection of NLX or NLXM in brain and plasma samples collected either two or 10 minutes after administration (**Fig 6A**). We show that neither dose of NLXM was detected within the central nervous system at either time point evaluated (**Figure 6B,C**). Furthermore, NLX was not detected in these NLXM-treated groups. In comparison, rats that received intravenous NLX exhibited significant, time-dependent detection of NLX in both plasma and brain samples (**Figure 6D**). We next evaluated cardiorespiratory changes from baseline in rats that received intravenous NLX or NLXM at either dose (**Fig S3A**). Data indicate that neither NLX nor NLXM significantly altered cardiorespiratory parameters relative to baseline (**Fig S3E-J**). Based on these findings, we utilized NLXM to further investigate the roles of peripheral MOR antagonism in the context of evaluating OIRD.

As shown in **Figure 2B-D and Figure S1B-D**, the responses evoked by 20 µg/kg and 50 µg/kg fentanyl induced an onset and duration of cardiorespiratory depression similar to **Figure 1**. As expected, NLX pretreatment completely blocked the decrease in cardiorespiratory parameters at both 20 µg/kg and 50 µg/kg doses of fentanyl. In rats that received 20 µg/kg fentanyl, 1 mg/kg NLXM pretreatment prevented bradycardic and hypoventilatory responses to fentanyl (**Figure 21-D**). For all parameters, saline-pretreated rats exhibited lower nadir values than NLX- and NLXM-pretreated rats, and there was no significant difference in the nadir or duration between NLX (1mg/kg) and NLXM (1mg/kg) pretreated rats that received 20 µg/kg

fentanyl (**Figure 2E-J**). Although there was a small drop in the nadir of oxygen saturation in NLXM-pretreated rats, this was not significantly different than NLX-pretreated animals (**Figure 2E**, p=0.2292). In rats that received 50 µg/kg fentanyl, 1 mg/kg NLXM pretreatment was unable to prevent the initial decrease in oxygen saturation and heart rate (**Fig S1E,G**). However, the duration of these responses was significantly shorter compared to saline-treated rats (**Figure S1F,H,J**). A higher dose of NLXM (5 mg/kg), which does not cross the blood brain barrier (**Figure 6D**), was then used in a separate group of animals that received 50 µg/kg fentanyl. Pretreatment with 5 mg/kg NLXM attenuated cardiorespiratory depression. While the nadir of oxygen saturation was significantly lower than NLX-pretreated rats, the duration of this effect was not significantly different between groups (**Figure S1E-J**). No sex differences were observed in the nadir or recovery time of any parameter (**Tables 3,4**). Together, these data demonstrate that peripheral MOR antagonism can sufficiently prevent OIRD by 20 µg/kg fentanyl-induced and strongly attenuates OIRD evoked by 50 µg/kg fentanyl.

Neuronal activation, as measured by Fos-IR, was examined in the nTS of rats pretreated with saline or opioid receptor antagonists followed by 20 µg/kg (**Figure 2K**) or 50 µg/kg fentanyl (**Figure S1K**). For fentanyl doses, saline pretreatment evoked the highest degree of Fos-IR in the nTS, including in a subpopulation of TH-IR neurons. Blocking peripheral MOR signaling with NLXM did not decrease fentanyl-induced nTS neuronal activation, while NLX, which blocks both central and peripheral MORs resulted in a significant reduction in nTS activation (**Figure 2L,M**). In rats that received the highest dose of fentanyl, the number of Fos-IR was similar between rats pretreated with saline and NLXM at both doses, with the only significant reduction occurring in NLX-pretreated animals (**Figure S1L**). This pattern of activation was also observed in catecholaminergic cells (**Figure S1M**), although around 30% of TH-IR neurons also displayed Fos-IR in NLX-pretreated rats.

**Peripheral opioid receptor antagonism reverses fentanyl-induced respiratory depression**

The above data demonstrate that peripheral MOR antagonism largely prevents fentanyl-induced respiratory depression without affecting nTS neuronal activation. Given that reversal of OIRD has more relevance as a therapeutic intervention, we next evaluated the extent to which NLXM reverses cardiorespiratory depression after it has been induced by 20 µg/kg (**Figure 3A**) and 50 µg/kg fentanyl (**Figure S2A**). Both 20 (**Figure 3B-D**) and 50 µg/kg fentanyl (**Figure S2B-D**) induced rapid decreases in oxygen saturation, heart rate and respiratory rate, similar to what was observed in **Figure 1**. The fentanyl-induced nadir in all physiological parameters prior to intravenous administration of saline and NLX or NLXM was similar between groups. In rats that

received 20 µg/kg fentanyl, both intravenous NLX (1 mg/kg) and NLXM (1 mg/kg) quickly restored cardiorespiratory values to baseline significantly faster than saline-pretreated animals (**Figure 3F,H,J**). This reversal of cardiorespiratory parameters was similar between NLX- and NLXM-treated animals. In rats that received 50 µg/kg fentanyl, NLX rapidly restored all physiological parameters to their baseline values (**Figure S2F,H,J**). While 1 mg/kg NLXM did not sufficiently reverse the OIRD induced by 50 µg/kg fentanyl (**Figure S2F**)**,** a higher dose of 5 mg/kg NLXM fully reversed the fentanyl-induced bradycardia and hypoventilation. The time to restore parameters to baseline was not significantly different to NLX. Importantly, this dose of NLXM is not detectable in the central nervous system (**Figure 5D**). We did not observe any sex differences in the nadir or recovery time of any parameter (**Tables 3,4**). Thus, blocking peripheral MORs sufficiently reverses OIRD at both moderate and high doses of fentanyl.

Because acute hypoxia activates nTS neurons (*24*), we investigated the impact of peripheral and central MOR antagonism on fentanyl-induced nTS neuronal activation (**Figure 3K**). At both doses of fentanyl administered, a similar degree of nTS neuronal activation was observed in all groups regardless of MOR antagonist administered after fentanyl (**Figure 3L,M; Figure S2L,M**). Together, these data demonstrate that selective antagonism of peripheral opioid receptors is sufficient to reverse cardiorespiratory depression induced by both moderate and high doses of fentanyl. Moreover, these data suggest that even a brief period of fentanyl-induced cardiorespiratory depression is sufficient to induce robust activation of nTS neurons, and this subsequent MOR antagonism has no additional effect to increase nTS activation.

**Reversal of Fentanyl-Induced Respiratory Depression with NLXM is not aversive**

NLX rapidly reverses OIRD, but produces unwanted side effects including the immediate onset of severe withdrawal (*12*, *13*). The intense symptoms induced during NLX-precipitated withdrawal present additional challenges in managing OUD in patients. Given that peripheral MOR antagonism sufficiently reverses fentanyl-induced cardiorespiratory depression to a degree that is comparable to NLX, we used a conditioned place aversion (CPA) approach to assess whether selective peripheral antagonism of MOR signaling produces aversive behaviors. Rats underwent a 3-session CPA challenge that consisted of pre-conditioning test, conditioning test, and post-conditioning test (**Figure 4A**). Horizontal locomotion in both compartments of the CPA boxes was assessed during both pre- and post-conditioning tests (**Figure 4B**). During the pre-conditioning test, rats exhibited no natural preference or aversion for either compartment. On the conditioning day (Day 2), a divider was placed in the middle of the CPA box. Rats received intravenous fentanyl (50 µg/kg) in their home cage. Four minutes later, rats were

placed into the paired compartment of the CPA box and immediately given intravenous saline (1 ml/kg), NLX (1 mg/kg) or NLXM (1 or 5 mg/kg). During the post-conditioning test, the divider was removed, and rats were allowed to explore both compartments of the CPA box. **Figure 4C** shows the time spent on the conditioned side of the CPA box for all groups. During the post-conditioning test, NLX-treated animals spent significantly less time in the NLX-paired compartment, suggesting that the reversal of OIRD on the conditioning day was aversive. This conditioned place aversion behavior was not observed in rats that received NLXM at either dose (**Figure 4D**). Importantly, a single conditioning session with fentanyl administered in the home cage followed by saline in the compartment instead of a MOR antagonist did not produce a preference or aversion to the saline-paired compartment. To rule out any potential effects of endogenous opioids influencing the behavioral responses to opioid receptor antagonism, we performed an additional test in which rats were given saline in their home cage, followed by NLX or NLXM in one of the CPA compartments (**Figure 4E,F**). Neither antagonist produced a preference nor aversion to the MOR antagonist-paired compartment (**Figure 4G**). There was no difference in CPA scores between these groups (**Figure 4H**). These findings are consistent with our data demonstrating that NLX and NLXM do not alter physiological parameters from baseline (**Figure S3**).

**Fentanyl induces a biphasic pattern of activity in nTS neurons**

As shown in **Figure 1**, fentanyl induced robust Fos-IR expression in the nTS. While Fos-IR quantification provides insight into the anatomical activation of brainstem subregions in response to fentanyl administration and OIRD reversal, this approach does not provide any temporal resolution of the activity of these cells. Therefore, we used wireless *in vivo* fiber photometry to assess dynamic changes in nTS calcium transient activity after intravenous fentanyl administration in anesthetized rats (**Figure 5A**). Catheterized rats underwent bilateral injections of an AAV expressing a calcium sensor (pGP-AAV-syn-jGCaMP8m-WPRE) into the nTS. On the day of the experiment, an optic fiber was lowered on the surface of the brainstem above the nTS and calcium transient activity was recorded (**Figure 5B**). GCaMP viral expression was observed throughout the caudal-rostral extent of the nTS in all rats (**Figure 5C**). Fentanyl (20 µg/kg) infusion induced a biphasic pattern of activity in the nTS, characterized by an initial robust increase in activity (Early Response) followed by a decrease below baseline (Late Response, **Figure 5D**). Pretreatment with NLXM (5 mg/kg) attenuated both phases of the fentanyl-induced changes in neuronal activity. As shown in **Figure 5E**, the area under the cure (AUC) was significantly elevated during the Early and Late Responses after fentanyl. In

contrast, no significant fentanyl-induced change in AUC was observed in NLXM-pretreated rats at either time point, indicating that changes in fentanyl-induced nTS neuronal activity are strongly mediated by peripheral MORs. We next examined the extent to which MOR antagonists restore the fentanyl-induced reductions in activity. After MOR antagonist administration, fentanyl-induced suppression of nTS activity returned to baseline during the early recovery in rats that received NLX, but not NLXM. However, both NLX and NLXM enhanced nTS activity above baseline during the late recovery period (**Figure 5F,G).** During the Late Recovery period, nTS activity was significantly enhanced above baseline in both NLX and NLXM-treated animals. Together, these data demonstrate that peripheral MOR antagonism is sufficient to reverse the fentanyl-induced decrease in nTS neuronal activity.

# DISCUSSION

OIRD is a complex problem that continues to be at the forefront of the opioid epidemic (*1*, *36*). The increased potency and faster onset of synthetic opioids like fentanyl has been attributed to the rising wave of opioid-related deaths in the US (*2*, *11*). Numerous studies have evaluated opioid-induced dysfunction within key regulatory sites in the central nervous system that contribute to the severity of OIRD (*1*, *15*, *16*, *18*, *28*). Peripheral MORs have also been examined for their roles in impacting OIRD (*12*, *33*). However, the specific contributions of central and peripheral MORs to the onset and duration of fentanyl-induced cardiorespiratory depression, along with the role of the nTS in these effects, are not completely understood. In this study, we show that blocking peripheral MORs with NLXM sufficiently prevents and reverses fentanyl-induced cardiorespiratory depression and systemic hypoxia. Furthermore, we demonstrate that peripheral opioid receptors mediate fentanyl-induced activity of nTS neurons. These data suggest that the nTS may be an area impacted by fentanyl via peripheral MOR activation. Lastly, we demonstrate that in addition to reversing fentanyl-induced cardiorespiratory depression, NLXM does not induce aversive behaviors, as compared to NLX. Together, these findings provide evidence that peripheral MOR antagonism may be a potential novel target to reverse OIRD without inducing withdrawal, anxiety, and aversion, all of which can contribute to further relapse in drug-seeking behaviors (*2*, *13*).

While numerous studies have focused on evaluating the effects of opioids acting at MORs present within brainstem and pontine networks, less attention has been given to identifying peripheral MOR mechanisms contributing to OIRD. NLX is the most common reversal agent used to treat OIRD (*13*, *36*). In addition to reversing opioid-induced analgesia,

NLX precipitates withdrawal symptoms and aversion in humans and rodents (*12*, *13*, *37*, *38*). In this study, we demonstrate that NLX-mediated reversal of OIRD caused a conditioned place aversion, as shown by a significant decrease in time spent in the NLX-associated compartment. This is likely the result of the induction of withdrawal symptoms that occur following antagonism of MOR in central reward pathways (*12*, *13*, *39*). In contrast, this aversive response was not observed in rats that received NLXM. These data suggest that alleviating fentanyl-induced respiratory distress without antagonizing central MOR may mitigate the aversive state produced by NLX.

Conditioned place preference and aversion paradigms have been utilized to evaluate rewarding and aversive properties of opioids and antagonists(*40–42*). Overall, we observed relatively minimal sex differences in basal and fentanyl-induced changes in cardiorespiratory depression, which is consistent with a previous report showing that sex differences due to fentanyl are relatively minimal compared to other opioids such as heroin(*9*). Previous reports have shown sexually dimorphic differences in fentanyl-induced conditioned place preference, with higher doses of fentanyl affecting females only(*42*). In present study, we administered fentanyl to male and female rats in the home cage followed by saline in the CPA box and observed neither a preference nor aversion in either sex. This suggests that the results obtained during OIRD-mediated reversal via NLX or NLXM are driven by effects within the CPA box and are not influenced by the rewarding properties of fentanyl itself. While previous reports have shown that NLX can be detected centrally after a subcutaneous injection of NLXM (*32*), we report here that no detectable amount of NLX or NLXM was found in brain tissue at the doses used in these studies (1 and 5 mg/kg, intravenous). Our data demonstrate robust fentanyl-induced neuronal activation in the nTS that appears to be mediated via peripheral MORs. Given the proximity of the nTS to the circumventricular organ area postrema(*43*), this raises the possibility that fentanyl can access the central nervous system via the area postrema to influence neuronal activation. However, our data showing the lack of a conditioned place aversion following NLXM-mediated reversal of OIRD support our biodistribution data showing no NLXM detection in brain samples that the observed effects primarily involve fentanyl actions at MOR located in peripheral sites. Similar to NLX, peripheral MOR antagonism with NLXM has been shown to partially reverse opioid-induced analgesia (*12*, *44*) which may pose limitations for pain management. While we report no changes in cardiorespiratory parameters from baseline following intravenous administration of NLX or NLXM in drug-naïve animals, previous work has shown that high doses of NLX elicit behavioral and physiological changes in humans, including cognitive impairment, nausea, tachycardia and hypertension, even at low and moderate doses

(*14*, *45*, *46*). Future investigations are needed to evaluate mechanisms underlying the therapeutic potential of NLXM as an intervention for managing OIRD in patients with OUDs.

The nTS is a region with a high degree of MOR expression, and appears to be primarily located on afferent fibers arising from the vagus nerve (*7*, *25*, *47*). While MOR has been shown to be present in nTS somas and dendrites (*25*, *28*), these MOR-expressing cells do not express Fos following exposure to opioids or hypoxia (*28*), which suggests a mechanism of presynaptic action of MOR signaling in the nTS. Likewise, the nodose ganglion (NG), which contains the cell bodies of nTS-projecting vagal sensory afferents, has high expression of MOR (*31*), and intra-nodose injection of fentanyl induces hypoventilation, although to a much lesser degree compared to systemic fentanyl (*48*).

In the present study, we used fiber photometry to characterize nTS neuronal responses to show that fentanyl induces an initial excitatory response in nTS cells. However, this response was short-lasting compared to the subsequent decrease in activity below baseline, suggesting that the primary effect of MOR signaling produce generalized inhibition of nTS neurons. This prolonged suppression of nTS neuronal activity may contribute to the overall duration of OIRD. Furthermore, our photometry data demonstrate that while the NLXM-mediated reversal of fentanyl-induced inhibition of nTS neurons was slower compared to NLX, activity was eventually restored. A similar finding was observed in OIRD experiments, as NLXM induced a rate of recovery in all parameters that was comparable to NLX. Taken together, this suggests that peripheral MOR antagonism may sufficiently override simultaneous central effects of fentanyl acting at MOR present in cardiorespiratory nuclei, including the nTS.

It is important to note that while all our experiments assessing fentanyl-induced cardiorespiratory depression were conducted in conscious rats breathing room air, photometry experiments were performed under isoflurane anesthesia. Due to the location of the nTS, chronic fiber implantation and subsequent in vivo photometry recordings in conscious, unrestrained animals is not possible. In the nTS, Isoflurane has been reported to suppress visceral afferent glutamatergic transmission and enhance GABAergic transmission via postsynaptic mechanisms (*49*), as well as induce cFos expression in the nTS (*50*). Precautions were taken to use the lowest dose of isoflurane needed to maintain sufficient anesthesia. However, we cannot rule out the possible influence of isoflurane anesthesia to influence the observed biphasic responses evoked by fentanyl. Nevertheless, our data support a mechanism by which fentanyl induces OIRD via disruption of visceral afferent signaling to the nTS, thereby leading to prolonged OIRD due to suppression of physiological reflex responses that would be normally engaged in response to systemic hypoxia.

The nTS plays an essential role in the regulation of basal-and reflex-evoked cardiorespiratory function (*22*). Activation of MOR in the nTS has been shown to blunt hypoxic ventilatory responses following MOR agonism in the nTS (*7*). Our data are consistent with previous work demonstrating opioid-induced activation of nTS neurons (*28*). The degree of fentanyl induced Fos-IR in the nTS resembles what is observed after acute exposure to hypoxic air (20, 46). Interestingly, we also observed increased Fos in the nTS at a dose of fentanyl that was below the threshold to induce respiratory depression. It is unclear whether the Fos-IR observed after low or high doses of fentanyl is, in part, the result of increased glutamatergic transmission stemming from enhanced chemoreceptor afferent signaling to the nTS or via MOR signaling within the nTS itself.

Glutamate is the primary neurotransmitter released from sensory afferent fibers into the nTS (*22*, *51*). While intra-nTS application of opioid agonists have been shown to reduce glutamate release and calcium channels via presynaptic mechanisms (*52*, *53*), opioids also have been shown to induce a similar biphasic action of Ca2+-dependent spikes in the nodose ganglion (*54*) that resembles what we observed in GCaMP-expressing nTS cells after intravenous fentanyl. NLXM strongly attenuated the fentanyl-induced excitatory wave observed in GCaMP-expressing nTS neurons, suggesting that MOR-expressing peripheral afferents mediate this transient activation of nTS neurons, even if the primary effect of fentanyl is to inhibit the nTS and suppress cardiorespiratory reflex function.

One possibility is that the increase in nTS activity may be mediated by opioid-induced disinhibition within the nTS. The nTS contains a large population of second order GABAergic interneurons that receive direct inputs from visceral afferents (*55*), and hypoxia activates these cells(*23*). nTS MOR agonists suppress the activity of these cells, primarily via presynaptic mechanisms (*56*), although postsynaptic mechanisms have been reported (*57*). Similarly, visceral afferents also activate catecholaminergic nTS neurons (*58*), which are critical for the generation of hypoxia-evoked cardiorespiratory responses(*34*, *59*). Opioids inhibit visceral afferent transmission to this cell group, primarily via a presynaptic mechanism (*52*). In the present study, we observed robust Fos expression in these cells at all doses of fentanyl examined. These findings raise the possibility that nTS dysfunction, via MOR-expressing peripheral inputs that terminate within this region, represents the first central site of fentanyl-induced dysfunction, ultimately leading to downstream effects in other brain regions that contribute to diminished autonomic and cardiorespiratory responses that contribute to the duration of OIRD.  Future studies are needed to fully evaluate the exact opioid-MOR effects in

the nTS, including specific MOR afferent inputs and the nTS phenotypes, to determine their relative contributions to OIRD.

In summary, these studies highlight a significant involvement of peripheral MORs contribute to the rapid cardiorespiratory depression induced by intravenous fentanyl. We have provided extensive characterization into how fentanyl elicits cardiorespiratory depression and examined the relationship between peripheral MORs and nTS activity in contributing to the duration of OIRD. Moreover, our findings suggest that selectively blocking peripheral opioid receptors could be a promising therapeutic strategy for managing OIRD. Notably, peripheral opioid receptor antagonists are already prescribed for patients undergoing chemotherapy to alleviate side effects such as opioid-induced constipation (*60*, *61*). Importantly, our data demonstrate that peripheral MOR antagonism appears to reverse OIRD without triggering unwanted effects of withdrawal that occur following NLX administration, suggesting that peripheral MOR antagonists like NLXM could potentially be utilized in treatment strategies for managing patients with OUD.

## Materials and Methods:

All surgical and experimental procedures were approved by Washington University Committee in accordance with the National Institutes of Health Guidelines for the Care and Use of Laboratory Animals and Animal Research: Reporting In Vivo Experiments (ARRIVE) guidelines. Rats were initially group-housed with two to three animals per cage on a 12/12-h dark/light cycle (lights on at 7:00) and acclimated to the animal facility holding rooms for at least 7 days before any manipulation. Following catheterization surgery, rats were single-housed and remained on an identical 12/12-h dark/light cycle. The temperature for the holding rooms of all animals ranged from 21 to 24 °C while the humidity was between 30 and 70%. Rats received food and water ad libitum for the duration of all experiments. All experiments were performed during the light cycle. For all experiments, male and female Sprague Dawley rats (250-350g) were used. In all data sets, male rats are represented by filled symbols and female rats are represented by open symbols.

**IV catheterization procedure:**

Animals were deeply anesthetized using Isoflurane (3% induction, 2% maintenance). A small incision was made in the dorsal surface of the neck. Another small incision was made on the ventral surface of the neck, and underlying tissue was carefully dissected to expose the jugular vein. An indwelling catheter was inserted into the jugular vein and sutured in place using non-absorbable silk suture. The catheter was then tunneled subcutaneously and exited the body through the first small hole in neck on the dorsal side. The ventral incision was closed using

non-absorbable silk suture. The exposed catheter was connected to a backpack device (Instech) containing a port for drug administration. Animals were given Carprofen (2 mg/kg sc), Baytril (8 mg/kg sc) and bupivacaine (5 mg/kg, site of incision). In addition, rats were given Carprofen tablets (Bio Serv, MD150-2) for 2 days after surgery to assist in wound healing and analgesia. Rats were singly housed following surgery and were allowed to recover for one week prior to the commencement of experiments. Catheter patency was maintained with daily flushing of 0.3 mL sterile saline containing gentamicin (1.33 mg/mL, i.v.)

**Respiratory depression experiments:**

Following recovery from IV catheterization surgery, conscious, freely moving rats in their home cages were fitted with a non-invasive pulse oximeter collar (Starr LifeSciences). Cardiorespiratory parameters (oxygen saturation, heart rate and respiratory rate) were collected (MouseOx v2.0, Starr LifeSciences) at baseline conditions in animals breathing room air, and after intravenous administration of fentanyl citrate (2, 20 or 50 µg/kg). A subset of animals received weight-adjusted intravenous administration of the nonselective opioid receptor antagonist naloxone hydrochloride (NLX; 1 mg/kg; Sigma 51481-60-8) or the peripherally restricted opioid receptor antagonist naloxone methiodide (NLXM; 1 or 5 mg/kg; Sigma N129) before or after fentanyl administration. Cardiorespiratory parameters were then measured for up to 60 minutes. For all OIRD experiments, the time course graphs consist of 30 seconds of data averaged into a single data point. The nadir was defined as the lowest point measured after fentanyl administration (for all graphs, red arrow indicates time of fentanyl administration, time=0 minutes). In addition, the recovery rate was defined as the time to reach 90% baseline of pre-fentanyl values for each cardiorespiratory parameter. Two hours after fentanyl administration, rats were transcardially perfused with 0.01M PBS followed by paraformaldehyde (4% in 0.01M PBS). Brains were removed and stored overnight at 4°C in 4% paraformaldehyde for post-fixation, followed by at least 72 h incubation in sucrose (30% in 0.01M PBS) solution. Isopentane was used to flash-freeze brains. Brainstem sections containing the nTS were sliced in the coronal plane (40 µm) using a cryostat (Leica CM 1950).

**Biodistribution**

A subset of previously catheterized drug-naïve rats was deeply anesthetized and then received intravenous administration of NLX (1 mg/kg) or NLXM (1 or 5 mg/kg). While still under anesthesia, rats were quickly decapitated two or ten minutes after intravenous administration of MOR antagonists. MOR antagonists were dosed in all rats at an experimentally relevant concentration with triplicate blood and brain samples collected at two time points. The early time point at 2 minutes evaluated conditions when the plasma concentration of the OR antagonist is

high and reflects the identical time point of intravenous administration for OIRD pretreatment experiments. The second collection time point (10 minutes) was intended to evaluate steady-state conditions and represent physiological experiments when reversal of OIRD was achieved by both antagonists. Brains were quickly removed and flash frozen in liquid nitrogen. Trunk blood was collected into capillary collection tubes containing lithium heparin (Greiner Bio-One; Fisher Scientific). The blood was spun on a centrifuge for 10 min at 4 °C, and plasma was carefully extracted from the supernatant. Brains and plasma samples underwent PK analyses for detection of NLX or NLXM at both time points. Standard rat PK studies dosed the candidate MOR antagonists and sample blood over multiple time points. A general description of tissue distribution can be obtained during PK modeling by calculating the volume of distribution. Samples underwent a direct measurement of peripheral restriction by measuring compound concentration in plasma and brain.

**Conditioned Place Aversion**

The aversive effects following reversal of OIRD were measured using Conditioned Place Aversion (CPA) (*62*). During a pre-conditioning session (Day 1), rats were allowed to explore both sides of a two compartment CPA box for 15 minutes. On the Conditioning Day (Day 2), a divider was placed in the middle of the box to restrict movement to one side on the box. Rats were then randomly assigned to one side of the CPA box, and this side was paired with either saline (1 ml/kg), NLX (1 mg/kg) or NLXM (1 or 5 mg/kg). Rats were given intravenous fentanyl (50 µg/kg) or saline in their home cages. Four minutes later, they were placed in the paired side of the box and immediately given saline or a MOR antagonist. Rats were confined to this compartment for 15 minutes. For all CPA experiments, measures were taken to balance the side of CPA box by drug and by sex. On the post-conditioning test (Day 3), the divider was removed. Rats were then placed in the CPA box and allowed to explore both sides of the CPA box for 15 minutes. The total time spent in the paired chamber and CPA scores were calculated for all groups.

**In vivo Fiber Photometry**

To selectively measure nTS neuronal calcium transient activity, we injected an AAV containing a calcium sensor expressed under the synapsin promoter (pGP-AAV-syn-jGCaMP8m-WPRE) into the nTS (500 nl per side; 0.3-0.5 mm anterior, ± 0.4 mm lateral and 0.4 mm ventral to brain surface, relative to calamus scriptorius). Rats were allowed at least 3 weeks to recover from nanoinjection surgery to allow for robust viral expression in the nTS before IV catheters were implanted as described above. On the day of the experiment, rats were deeply anesthetized with isoflurane (3-4% induction, 2% maintenance), placed in the stereotaxic apparatus, and the

nTS was exposed as described above. To overcome limitations associated with chronic fiber implants in the nTS, a wireless photometry headstage (TeleFipho, Amuza Inc.) was secured to a 5 mm flat-tipped silica optic fiber cannula (400 μm c.d./470 μm o.d., NA 0.37, 2.5 mm receptacle; Doric) and mounted the stereotaxic arm with an apparatus 3D printed in house to permit simultaneous nTS exposure and photometry recordings. The optic fiber was lowered to the site of the dorsal brainstem and firmly pressed on the surface above the nTS until a signal was detected (~0.3-0.5 mm ventral from the surface). An LED generated blue light was bandpass-filtered (445-490 nm) to excite jGCaMP8m and emission fluorescence was detected by an internal photodiode detector for green light (bandpass filtered at 500-550 nm). An internal DC amplifier transmitted the data (16-bit arbitrary unit; AU) to a wireless receiver (TeleFipho, Amuza Inc.) and the data was extracted in real-time using TeleFipho software (Amuza Inc.) at a sampling rate of 100 Hz. The offset was set to 90° and the LED power was adjusted to achieve an optimal signal output (30-40k a.u.) not to exceed 36 mW power, and remained constant throughout the recording. Baseline activity of GCaMP fluorescence nTS-infected cells was measured after at least 5 min to mitigate effects of baseline drift in signal due to slow photobleaching artifacts. Then, baseline activity was measured for at least 30 s prior to administration of either fentanyl (20 µg/kg, i.v.) or NLXM (5 mg/kg, i.v.). After response activity was recorded, rats received a second intravenous injection of either an opioid receptor antagonist (NLX,1 mg/kg or NLXM, 5 mg/kg) or fentanyl (20 µg/kg), respectively. Each intravenous administration was manually time locked to calcium transient recordings by a second experimenter and response activity following each injection was recorded for 60 s before administration of the second injection or conclusion of the experiment. Rats were transcardially perfused with PFA at the end of the experiment as described above and viral expression was validated for all animals.

For analysis of calcium transient activity, the raw data was fit to a double-exponential curve and subtracted from the raw data to account for any residual effects of baseline drift. Matlab Signal Analyzer was used to extract regions of interest (ROIs) in the signal in 90-s traces (30 s pre-treatment, 60 s post-treatment) and traces were aligned to the time of injection. ROIs were standardized as z-scores using the sample standard deviation, *S,* where $S = \sqrt{\frac{\Sigma_{i=1}^{n}(x_i - \bar{X})^2}{n-1}}$ such that signals were centered to have a mean of 0 and scaled to have a standard deviation of 1. Based on this, the area under the curve (AUC) of ROI z-scores were calculated in 30-s bins using the trapezoidal rule (*trapz* function in Matlab) and one-sample t-tests were used to determine differences relative to baseline (theoretical mean = 0). For presentation, transients

were down sampled by a factor of 10 with a phase offset of 2 and the resultant 10 Hz traces were smoothed using a moving mean duration of 5% of total ROI.

**Immunohistochemistry (IHC):**

Immunohistochemical procedures were performed as previously described (*63*). Brainstem sections containing the nTS were sliced using a cryostat (Leica) at a thickness of 40 um. Free-floating sections were rinsed in 0.01M PBS, blocked in 10% Normal Donkey Serum (Sigma) in 0.01M PBS-triton, and then incubated with the following antibodies: cFos (Rabbit anti-cFos; ab190289, Abcam; AB_2737414); Tyrosine Hydroxylase (TH, Mouse anti-TH; MAB318, Millipore; AB_2201528). The following day, sections were rinsed with 0.01M PBS, incubated with Donkey anti-Rabbit Cy3 and Donkey anti-Mouse Alexa fluor 488 (1:200; in 3% NDS and 0.3% Triton in 0.01M PBS) and used to visualize targets of interest (Jackson ImmunoResearch).

**Image acquisition:**

Immunoreactivity (IR) and viral expression were examined with a Leica DMR microscope at 20X magnification. 20 µm thick z-stacks of the nTS (2 µm per plane) were collected. ImageJ (v. 1.48, NIH) software was used for post-processing and analysis. In all groups, three sections of the nTS (corresponding to -360, 0, +360 µm relative to calamus scriptorius) were collected.

**Brainstem immunohistochemical analyses**

Using ImageJ software, the regions containing the nTS were outlined, and unilateral counts of Fos-IR, TH-IR and co-labeled Fos- and TH-IR neurons were performed using a custom-made plugin (Cell Counter) for each of the 3 nTS sections per animal. The total number of each phenotype was summed from these 3 sections, and the percentage of TH-IR cells co-expressing Fos-IR was determined.

**Statistics**

For all experiments, the normality of sample data was determined using D'Agostino and Pearson tests and Shapiro–Wilk tests. Statistical significance was taken as * $p<0.05$, ** $p<0.01$, *** $p<0.001$ and ****$p<0.0001$, as determined by two-way repeated measures analysis of variance (ANOVA) followed by Sidak's post hoc test; one-way ANOVA with Tukey post-hoc test, two-tailed unpaired t-test, two-tailed paired t-test, one sample t-test.

# References


1. J.-M. Ramirez, N. J. Burgraff, A. D. Wei, N. A. Baertsch, A. G. Varga, H. A. Baghdoyan, R. Lydic, K. F. Morris, D. C. Bolser, E. S. Levitt, Neuronal mechanisms underlying opioid-induced respiratory depression: our current understanding. *Journal of Neurophysiology* **125**, 1899–1919 (2021).

2. S. D. Comer, C. M. Cahill, Fentanyl: Receptor pharmacology, abuse potential, and implications for treatment. *Neuroscience & Biobehavioral Reviews* **106**, 49–57 (2019).

3. C. L. Mattson, Trends and Geographic Patterns in Drug and Synthetic Opioid Overdose Deaths — United States, 2013–2019. *MMWR Morb Mortal Wkly Rep* **70** (2021).

4. S. Parida, J. P. De Aquino, M. Sofuoglu, High potency synthetic opioids: Curbing the third wave of the opioid crisis. *Neuroscience & Biobehavioral Reviews* **106**, 9–10 (2019).

5. N. Wilson, M. Kariisa, P. Seth, H. Smith, N. L. Davis, Drug and Opioid-Involved Overdose Deaths — United States, 2017–2018. *MMWR Morb Mortal Wkly Rep* **69**, 290–297 (2020).

6. A. Mansour, C. A. Fox, S. Burke, F. Meng, R. C. Thompson, H. Akil, S. J. Watson, Mu, delta, and kappa opioid receptor mRNA expression in the rat CNS: An in situ hybridization study. *Journal of Comparative Neurology* **350**, 412–438 (1994).

7. J. Zhuang, X. Gao, F. Gao, F. Xu, Mu-opioid receptors in the caudomedial NTS are critical for respiratory responses to stimulation of bronchopulmonary C-fibers and carotid body in conscious rats. *Respir Physiol Neurobiol* **235**, 71–78 (2017).

8. R. Hill, R. Santhakumar, W. Dewey, E. Kelly, G. Henderson, Fentanyl depression of respiration: Comparison with heroin and morphine. *Br J Pharmacol* **177**, 254–265 (2020).

9. R. C. N. Marchette, E. R. Carlson, E. V. Frye, L. E. Hastings, J. C. M. Vendruscolo, G. Mejias-Torres, S. J. Lewis, A. Hampson, N. D. Volkow, L. F. Vendruscolo, G. F. Koob, Heroin- and Fentanyl-Induced Respiratory Depression in a Rat Plethysmography Model: Potency, Tolerance, and Sex Differences. *J Pharmacol Exp Ther* **385**, 117–134 (2023).

10. T. Lewanowitsch, R. J. Irvine, Naloxone and its quaternary derivative, naloxone methiodide, have differing affinities for mu, delta, and kappa opioid receptors in mouse brain homogenates. *Brain Res* **964**, 302–305 (2003).

11. N. Fairbairn, P. O. Coffin, A. Y. Walley, Naloxone for heroin, prescription opioid, and illicitly made fentanyl overdoses: Challenges and innovations responding to a dynamic epidemic. *International Journal of Drug Policy* **46**, 172–179 (2017).

12. T. Lewanowitsch, R. J. Irvine, Naloxone methiodide reverses opioid-induced respiratory depression and analgesia without withdrawal. *European Journal of Pharmacology* **445**, 61–67 (2002).

13. J. T. Lai, C. E. Goldfine, B. P. Chapman, M. M. Taylor, R. K. Rosen, S. P. Carreiro, K. M. Babu, Nobody Wants to Be Narcan'd: A Pilot Qualitative Analysis of Drug Users' Perspectives on Naloxone. *West J Emerg Med* **22**, 339–345 (2021).

14. B. Yugar, K. McManus, C. Ramdin, L. S. Nelson, M. A. Parris, Systematic Review of Naloxone Dosing and Adverse Events in the Emergency Department. *The Journal of Emergency Medicine* **65**, e188–e198 (2023).

15. I. Bachmutsky, X. P. Wei, E. Kish, K. Yackle, Opioids depress breathing through two small brainstem sites. *eLife* **9**, e52694 (2020).

16. J. T. Bateman, E. S. Levitt, Opioid suppression of an excitatory pontomedullary respiratory circuit by convergent mechanisms. *eLife* **12**, e81119 (2023).

17. A. Haji, H. Yamazaki, Y. Ohi, R. Takeda, Distribution of μ receptors in the ventral respiratory group neurons; immunohistochemical and pharmacological studies in decerebrate cats. *Neuroscience Letters* **351**, 37–40 (2003).

18. E. S. Levitt, A. P. Abdala, J. F. R. Paton, J. M. Bissonnette, J. T. Williams, μ opioid receptor activation hyperpolarizes respiratory-controlling Kölliker–Fuse neurons and suppresses post-inspiratory drive. *The Journal of Physiology* **593**, 4453–4469 (2015).

19. B. Palkovic, V. Marchenko, E. J. Zuperku, E. A. E. Stuth, A. G. Stucke, Multi-Level Regulation of Opioid-Induced Respiratory Depression. *Physiology (Bethesda)* **35**, 391–404 (2020).

20. G. Montandon, W. Qin, H. Liu, J. Ren, J. J. Greer, R. L. Horner, PreBötzinger Complex Neurokinin-1 Receptor-Expressing Neurons Mediate Opioid-Induced Respiratory Depression. *J. Neurosci.* **31**, 1292–1301 (2011).

21. K. T. S. Pattinson, Opioids and the control of respiration. *British Journal of Anaesthesia* **100**, 747–758 (2008).

22. M. C. Andresen, D. L. Kunze, Nucleus tractus solitarius--gateway to neural circulatory control. *Annu Rev Physiol* **56**, 93–116 (1994).

23. T. L. King, C. M. Heesch, C. G. Clark, D. D. Kline, E. M. Hasser, Hypoxia activates nucleus tractus solitarii neurons projecting to the paraventricular nucleus of the hypothalamus. *American Journal of Physiology-Regulatory, Integrative and Comparative Physiology* **302**, R1219–R1232 (2012).

24. L. J. Teppema, J. G. Veening, A. Kranenburg, A. Dahan, A. Berkenbosch, C. Olievier, Expression of c-fos in the rat brainstem after exposure to hypoxia and to normoxic and hyperoxic hypercapnia. *Journal of Comparative Neurology* **388**, 169–190 (1997).

25. S. A. Aicher, A. Goldberg, S. Sharma, V. M. Pickel, μ-opioid receptors are present in vagal afferents and their dendritic targets in the medial nucleus tractus solitarius. *Journal of Comparative Neurology* **422**, 181–190 (2000).

26. A. Disney, K. M. Olson, A. M. Shafer, S. C. Moore, J. P. Anand, J. R. Traynor, S. M. Husbands, Opioid Antagonists from the Orvinol Series as Potential Reversal Agents for Opioid Overdose. *ACS Chem Neurosci* **13**, 3108–3117 (2022).

27. E. Solis, K. T. Cameron-Burr, Y. Shaham, E. A. Kiyatkin, Fentanyl-Induced Brain Hypoxia Triggers Brain Hyperglycemia and Biphasic Changes in Brain Temperature. *Neuropsychopharmacol.* **43**, 810–819 (2018).

28. S. N. Maletz, B. T. Reid, A. G. Varga, E. S. Levitt, Nucleus Tractus Solitarius Neurons Activated by Hypercapnia and Hypoxia Lack Mu Opioid Receptor Expression. *Front Mol Neurosci* **15**, 932189 (2022).

29. E. Salas, E. Alonso, M. J. Polanco, M. V. Cano, M. Ruiz-Gayo, L. F. Alguacil, Differential regulation of CDK5 and c-Fos expression by morphine in the brain of Lewis and Fischer 344 rat strains. *Neuroscience* **230**, 151–156 (2013).

30. P. J. Cabot, P. R. Dodd, T. Cramond, M. T. Smith, Characterization of non-conventional opioid binding sites in rat and human lung. *Eur J Pharmacol* **268**, 247–255 (1994).

31. J.-L. Li, T. Kaneko, N. Mizuno, Effects of peripheral nerve ligation on expression of μ-opioid receptor in sensory ganglion neurons: an immunohistochemical study in dorsal root and nodose ganglion neurons of the rat. *Neuroscience Letters* **214**, 91–94 (1996).

32. D. Perekopskiy, A. Afzal, S. N. Jackson, L. Muller, A. S. Woods, E. A. Kiyatkin, The Role of Peripheral Opioid Receptors in Triggering Heroin-induced Brain Hypoxia. *Sci Rep* **10**, 833 (2020).

33. F. Henderson Jr, W. J. May, R. B. Gruber, A. P. Young, L. A. Palmer, B. Gaston, S. J. Lewis, Low-dose morphine elicits ventilatory excitant and depressant responses in conscious rats: Role of peripheral μ-opioid receptors. *Open Journal of Molecular and Integrative Physiology* **3**, 111–124 (2014).

34. T. L. King, B. C. Ruyle, D. D. Kline, C. M. Heesch, E. M. Hasser, Catecholaminergic neurons projecting to the paraventricular nucleus of the hypothalamus are essential for cardiorespiratory adjustments to hypoxia. *Am J Physiol Regul Integr Comp Physiol* **309**, R721-731 (2015).

35. S. McGaraughty, P. Honore, C. T. Wismer, J. Mikusa, C. Z. Zhu, H. A. McDonald, B. Bianchi, C. R. Faltynek, M. F. Jarvis, Endogenous opioid mechanisms partially mediate P2X3/P2X2/3-related antinociception in rat models of inflammatory and chemogenic pain but not neuropathic pain. *Br J Pharmacol* **146**, 180–188 (2005).

36. J. T. Bateman, S. E. Saunders, E. S. Levitt, Understanding and countering opioid-induced respiratory depression. *British Journal of Pharmacology* **n/a** (2021).

37. J. Neale, J. Strang, Naloxone—does over-antagonism matter? Evidence of iatrogenic harm after emergency treatment of heroin/opioid overdose. *Addiction* **110**, 1644–1652 (2015).

38. A. Dahan, R. van der Schrier, T. Smith, L. Aarts, M. van Velzen, M. Niesters, Averting Opioid-induced Respiratory Depression without Affecting Analgesia. *Anesthesiology* **128**, 1027–1037 (2018).

39. M. J. Katovich, J. W. Simpkins, J. O'Meara, Effects of opiod antagonists and their quaternary analogs on temperature changes in morphine-dependent rats. *Life Sciences* **39**, 1845–1854 (1986).

40. J. M. Finlay, A. Jakubovic, A. G. Phillips, H. C. Fibiger, Fentanyl-induced conditional place preference: lack of associated conditional neurochemical events. *Psychopharmacology (Berl)* **96**, 534–540 (1988).

41. A. D. Gaulden, N. Burson, N. Sadik, I. Ghosh, S. J. Khan, S. Brummelte, S. Kallakuri, S. A. Perrine, Effects of fentanyl on acute locomotor activity, behavioral sensitization, and contextual reward in female and male rats. *Drug Alcohol Depend* **229**, 109101 (2021).

42. Z. T. Knauss, C. J. Hearn, N. C. Hendryx, F. S. Aboalrob, Y. Mueller-Figueroa, D. S. Damron, S. J. Lewis, D. Mueller, Fentanyl-induced reward seeking is sex and dose dependent and is prevented by D-cysteine ethylester. *Front. Pharmacol.* **14** (2023).

43. C. J. Price, T. D. Hoyda, A. V. Ferguson, The area postrema: a brain monitor and integrator of systemic autonomic state. *Neuroscientist* **14**, 182–194 (2008).

44. V. Spahn, G. Del Vecchio, D. Labuz, A. Rodriguez-Gaztelumendi, N. Massaly, J. Temp, V. Durmaz, P. Sabri, M. Reidelbach, H. Machelska, M. Weber, C. Stein, A nontoxic pain killer designed by modeling of pathological receptor conformations. *Science* **355**, 966–969 (2017).

45. MartinR. Cohen, RobertM. Cohen, D. Pickar, H. Weingartner, DennisL. Murphy, WilliamE. Bunney, Behavioural effects after high dose naloxone administration to normal volunteers. *The Lancet* **318**, 1110 (1981).

46. M. R. Cohen, R. M. Cohen, D. Pickar, D. L. Murphy, W. E. Bunney, Physiological effects of high dose naloxone administration to normal adults. *Life Sci* **30**, 2025–2031 (1982).

47. S. Nomura, Y.-Q. Ding, T. Kaneko, J.-L. Li, N. Mizuno, Localization of μ-opioid receptor-like immunoreactivity in the central components of the vagus nerve: A light and electron microscope study in the rat. *Neuroscience* **73**, 277–286 (1996).

48. Z. Zhang, C. Zhang, M. Zhou, F. Xu, Activation of Opioid μ-Receptors, but not δ- or κ-Receptors, Switches Pulmonary C-Fiber-Mediated Rapid Shallow Breathing into An Apnea in Anesthetized Rats. *Respir Physiol Neurobiol* **183**, 211–217 (2012).

49. J. H. Peters, S. J. McDougall, D. Mendelowitz, D. R. Koop, M. C. Andresen, Isoflurane Differentially Modulates Inhibitory and Excitatory Synaptic Transmission to the Solitary Tract Nucleus. *Anesthesiology* **108**, 675–683 (2008).

50. Y. Hu, J. T. Qi, Z. Zhang, M. Q. Luo, Y. W. Wang, Comparative Brain-Wide Mapping of Isoflurane and Ketamine-Activated Nuclei and Functional Networks. *eLife* **12** (2023).

51. W. T. Talman, M. H. Perrone, D. J. Reis, Evidence for L-glutamate as the neurotransmitter of baroreceptor afferent nerve fibers. *Science* **209**, 813–815 (1980).

52. R. J. Cui, B. L. Roberts, H. Zhao, M. C. Andresen, S. M. Appleyard, Opioids inhibit visceral afferent activation of catecholamine neurons in the solitary tract nucleus. *Neuroscience* **222**, 181–190 (2012).

53. H. Rhim, R. J. Miller, Opioid receptors modulate diverse types of calcium channels in the nucleus tractus solitarius of the rat. *J. Neurosci.* **14**, 7608–7615 (1994).

54. H. Higashi, P. Shinnick-Gallagher, J. P. Gallagher, Morphine enhances and depresses Ca2+-dependent responses in visceral primary afferent neurons. *Brain Research* **251**, 186–191 (1982).

55. T. W. Bailey, S. M. Appleyard, Y.-H. Jin, M. C. Andresen, Organization and properties of GABAergic neurons in solitary tract nucleus (NTS). *J Neurophysiol* **99**, 1712–1722 (2008).

56. A. J. Boxwell, Y. Yanagawa, S. P. Travers, J. B. Travers, The μ-opioid receptor agonist DAMGO presynaptically suppresses solitary tract-evoked input to neurons in the rostral solitary nucleus. *J Neurophysiol* **109**, 2815–2826 (2013).

57. N. R. Glatzer, B. N. Smith, Modulation of synaptic transmission in the rat nucleus of the solitary tract by endomorphin-1. *J Neurophysiol* **93**, 2530–2540 (2005).

58. S. M. Appleyard, D. Marks, K. Kobayashi, H. Okano, M. J. Low, M. C. Andresen, Visceral afferents directly activate catecholamine neurons in the solitary tract nucleus. *J Neurosci* **27**, 13292–13302 (2007).

59. C. S. Bathina, A. Rajulapati, M. Franzke, K. Yamamoto, J. T. Cunningham, S. Mifflin, Knockdown of tyrosine hydroxylase in the nucleus of the solitary tract reduces elevated blood pressure during chronic intermittent hypoxia. *Am J Physiol Regul Integr Comp Physiol* **305**, R1031–R1039 (2013).

60. E. Floettmann, K. Bui, M. Sostek, K. Payza, M. Eldon, Pharmacologic Profile of Naloxegol, a Peripherally Acting μ-Opioid Receptor Antagonist, for the Treatment of Opioid-Induced Constipation. *J Pharmacol Exp Ther* **361**, 280–291 (2017).

61. J. V. Pergolizzi, P. J. Christo, J. A. LeQuang, P. Magnusson, The Use of Peripheral μ-Opioid Receptor Antagonists (PAMORA) in the Management of Opioid-Induced Constipation: An Update on Their Efficacy and Safety. *Drug Des Devel Ther* **14**, 1009–1025 (2020).

62. T. M. Tzschentke, Measuring reward with the conditioned place preference (CPP) paradigm: update of the last decade. *Addict Biol* **12**, 227–462 (2007).

63. B. C. Ruyle, D. Martinez, C. M. Heesch, D. D. Kline, E. M. Hasser, The PVN enhances cardiorespiratory responses to acute hypoxia via input to the nTS. *Am J Physiol Regul Integr Comp Physiol* **317**, R818–R833 (2019).

## Acknowledgements

We wish to thank Justin Meyer for breeding the rat colonies that were used in these experiments and for general assistance throughout the experiments. We also thank Mike Cameron (Scripps Institute) for mass spectrometry experiments used for all biodistribution experiments. We also wish to thank Kristine Yoon and Thomas Schodl for their technical assistance.

## Author Contributions

Conceptualization: BCR NM and JAM

Methodology: BCR, NM and JAM

Formal analysis of all data: BCR, SM, RK, MT and JAH

Photometry acquisition and extraction: BCR and JAH

Respiratory depression experiments: BCR, SM, RK, MT, JM, CR, SAL

Conditioned Place Aversion: BCR, SM, MT, JM

Biodistribution experiments: BCR and TL

Immunohistochemistry, microscopy and cell counting: BCR, SM, RK, MT, JM, SAL

Catheterization surgeries: BCR, SM, RK, MT, JM, SAL

Writing of original draft: BCR

Writing (review and editing): BCR, RK, JM, SAL, TL, JAH, NM, JAM

Funding Acquisition, BR, JM

Resources: JM

Supervision: BR and JM

## Data Availability Statement

The authors confirm that all relevant data are included in the paper and its Supplementary Information files. All data generated in this study are provided in the Supplementary Information/Source Data file. Further information and requests for resources and reagents should be directed to and will be fulfilled by the Lead Contact, Jose A. Morón (jmoron-concepcion @wustl.edu).

## Competing Interests

We have no competing interests to declare.

## Funding:

National Institute of Health grant R01DA042499 (JMC)

National Institute of Health grant R01DA045463 (JMC)

National Institute of Health grant R01DA054900(JMC)

National Institute of Health grant R56DA059067 (JMC)

Washington University McDonnell Small Grants Program GF0012452 (BCR)

National Institute of Health grant T32DA007261 (BCR)

National Institute of Health grant S10OD030332-01(Michael Cameron, Scripps Research)

# FIGURES

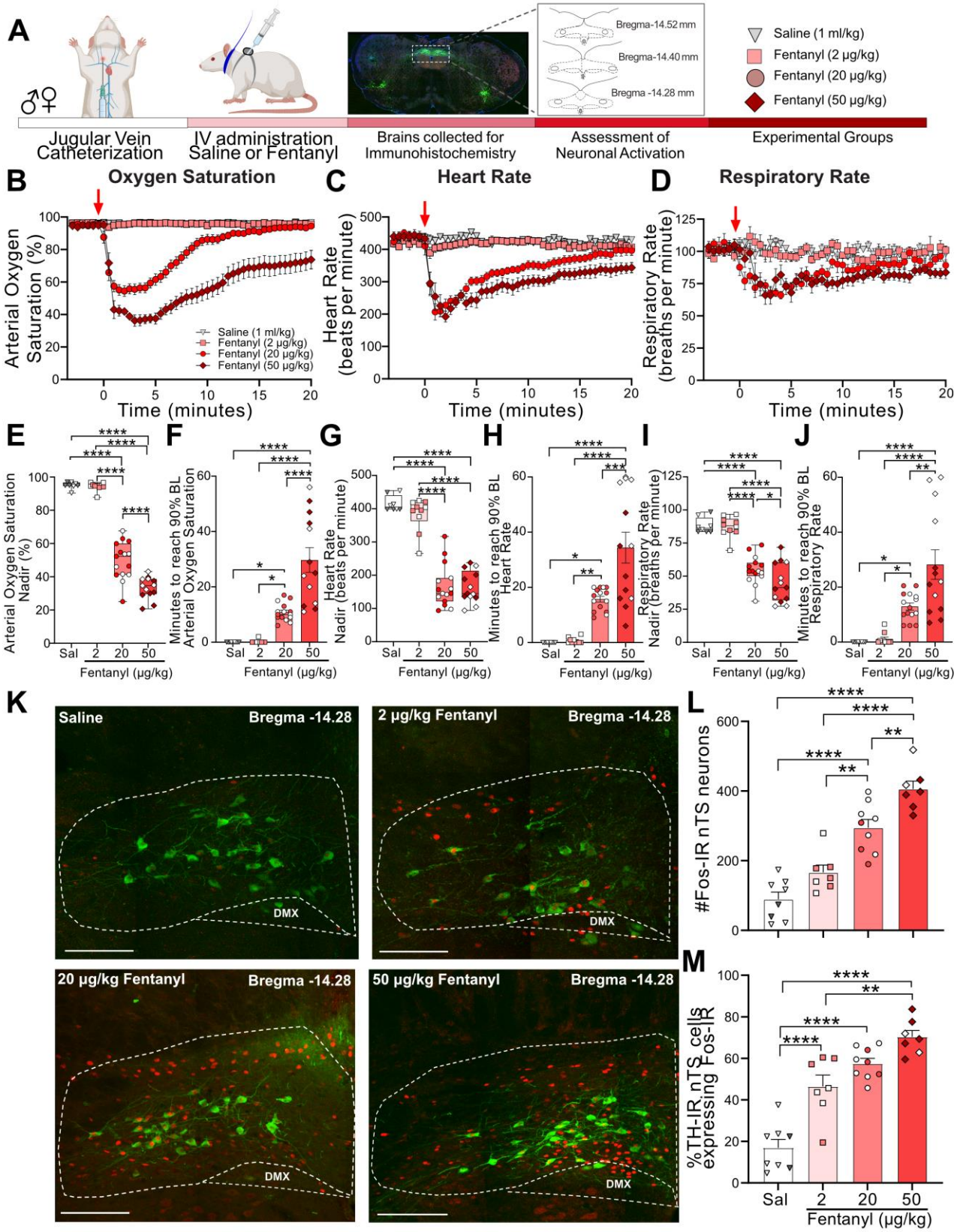
A
Bregma-14.52 mm
Bregma-14.40 mm
Bregma -14.28 mm
Saline (1 ml/kg)
Fentanyl (2 µg/kg)
Fentanyl (20 µg/kg)
Fentanyl (50 µg/kg)
Jugular Vein Catheterization
IV administration Saline or Fentanyl
Brains collected for Immunohistochemistry
Assessment of Neuronal Activation
Experimental Groups
B Oxygen Saturation
Arterial Oxygen Saturation (%)
Time (minutes)
C Heart Rate
Heart Rate (beats per minute)
D Respiratory Rate
Respiratory Rate (breaths per minute)
E Arterial Oxygen Saturation Nadir (%)
F Minutes to reach 90% BL Arterial Oxygen Saturation
G Heart Rate Nadir (beats per minute)
H Minutes to reach 90% BL Heart Rate
I Respiratory Rate Nadir (breaths per minute)
J Minutes to reach 90% BL Respiratory Rate
Sal 2 20 50
Fentanyl (µg/kg)
K
Saline Bregma -14.28
2 µg/kg Fentanyl Bregma -14.28
20 µg/kg Fentanyl Bregma -14.28
50 µg/kg Fentanyl Bregma -14.28
DMX
L #Fos-IR nTS neurons
M %TH-IR nTS cells expressing Fos-IR

**Figure 1: Fentanyl induces cardiorespiratory depression and nTS neuronal activation in a dose-dependent manner**

**A.** Schematic showing the timeline for OIRD collar experiments. Male and Female SD rats underwent jugular catheterization surgery. The following week, conscious rats in their home cages were fitted with a pulse oximeter collar and received intravenous administration of either saline (n=8, triangles) or fentanyl (2 µg/kg: (n=10, squares); 20 µg/kg, (n=15, circles); 50 µg/kg, (n=13, diamonds). Baseline cardiorespiratory parameters were measured for 3 minutes prior to IV administration and up to 60 minutes after saline or fentanyl. At the conclusion of experiments, brains were collected from a subset of animals in each group and processed for Fos- and TH-immunoreactivity. Time course data showing oxygen saturation (**B**), heart rate (**C**) and respiratory rate (**D**) data measurements collected in all groups before and after saline or fentanyl. Changes in oxygen saturation were assessed as nadir (lowest value; **E,G,I**) and time to recover to 90% of baseline (pre-saline/fentanyl; **F,H,J**) administration. There was a dose-dependent decrease in the nadir for oxygen saturation (One-way ANOVA, $F_{(3,42)} = 186.3$, $p < 0.0001$; Tukey's post-hoc ****$p<0.0001$), heart rate (One-way ANOVA $F_{(3, 42)} = 74.93$, $p < 0.0001$; Tukey's post-hoc ****$p<0.0001$) and respiratory rate (One-way ANOVA, $F_{(3, 42)} = 45.60$, $p < 0.0001$; Tukey's post-hoc ****$p<0.0001$, *$p<0.05$). Time to recover to 90% baseline Oxygen Saturation (One-way ANOVA, $F_{(3, 42)} = 28.72$, $p < 0.0001$; Tukey's post-hoc ****$p<0.0001$, *$p<0.05$) heart rate (One-way ANOVA, $F_{(3, 42)} = 23.89$, $p < 0.0001$; Tukey's post-hoc ****$p<0.0001$, ***$p<0.001$, **$p<0.01$, *$p<0.05$) and respiratory rate (One-way ANOVA, $F_{(3, 42)} = 16.53$, $p<0.0001$; Tukey's post-hoc ****$p<0.0001$, **$p<0.01$, *$p<0.05$). **K.** Merged photomicrographs of coronal brainstem sections displaying representative Fos- and TH-immunoreactivity in the nTS of rats that received intravenous saline or fentanyl. Scale bar = 200 µm. **L.** Mean data show that 20 and 50 µg/kg fentanyl induced a significantly greater number of Fos-IR cells in the nTS compared to saline and 2 µg/kg fentanyl. (One-way ANOVA, $F_{(3,27)} = 37.13$, $p < 0.0001$; Tukey's post hoc ****$p<0.0001$, **$p<0.001$) **M.** Mean data showing the percentage of TH-IR nTS neurons expressing Fos-IR. Rats that received 2 µg/kg fentanyl displayed a significantly higher increase in activated TH-IR neurons compared to saline-treated rats. Both 20 and 50 µg/kg fentanyl induced a significantly higher percentage of activation in TH cells compared to saline and 2 µg/kg fentanyl. (One-way ANOVA, $F_{(3,27)} = 37.13$, $p<0.0001$; Tukey's post-hoc ****$p<0.0001$, **$p<0.01$)

825

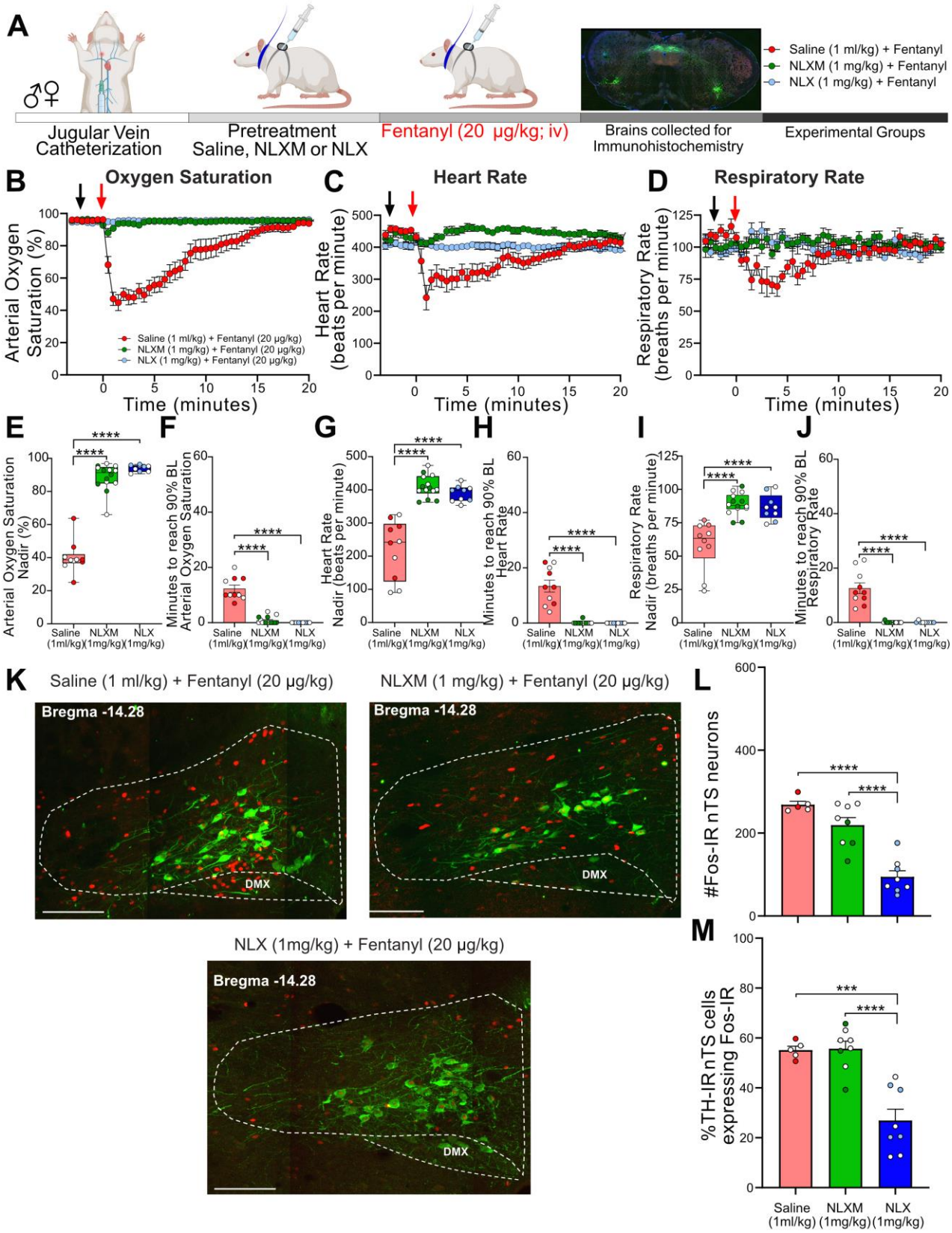
A
♂♀
Jugular Vein Catheterization
Pretreatment Saline, NLXM or NLX
Fentanyl (20 µg/kg; iv)
Brains collected for Immunohistochemistry
Experimental Groups
Saline (1 ml/kg) + Fentanyl
NLXM (1 mg/kg) + Fentanyl
NLX (1 mg/kg) + Fentanyl
B Oxygen Saturation
Arterial Oxygen Saturation (%)
Saline (1 ml/kg) + Fentanyl (20 µg/kg)
NLXM (1 mg/kg) + Fentanyl (20 µg/kg)
NLX (1 mg/kg) + Fentanyl (20 µg/kg)
Time (minutes)
C Heart Rate
Heart Rate (beats per minute)
Time (minutes)
D Respiratory Rate
Respiratory Rate (breaths per minute)
Time (minutes)
E
Arterial Oxygen Saturation Nadir (%)
F
Minutes to reach 90% BL Arterial Oxygen Saturation
G
Heart Rate Nadir (beats per minute)
H
Minutes to reach 90% BL Heart Rate
I
Respiratory Rate Nadir (breaths per minute)
J
Minutes to reach 90% BL Respiratory Rate
Saline (1ml/kg)
NLXM (1mg/kg)
NLX (1mg/kg)
K
Saline (1 ml/kg) + Fentanyl (20 µg/kg)
NLXM (1 mg/kg) + Fentanyl (20 µg/kg)
NLX (1mg/kg) + Fentanyl (20 µg/kg)
Bregma -14.28
DMX
L
#Fos-IR nTS neurons
M
%TH-IR nTS cells expressing Fos-IR

826

**Figure 2. NLXM attenuates respiratory depression without affecting nTS neuronal activation induced by 20 µg/kg fentanyl: A.** Schematic showing the timeline for OIRD collar experiments. Male and Female SD rats underwent jugular catheterization surgery. The following week, conscious rats in their home cages received intravenous administration (pretreatment) of either saline (1 ml/kg; n=10), NLX (1 mg/kg; n=9) or NLXM (1 mg/kg; n=15). Two minutes later, all rats received intravenous fentanyl (20 µg/kg). Cardiorespiratory parameters were measured up to 60 minutes after fentanyl. At the conclusion of the experiment, brains were collected from a subset of animals in each group and processed for Fos- and TH- immunoreactivity. Time course data showing oxygen saturation (**B**), heart rate (**C**) and respiratory rate (**D**) data measurements collected in all groups before and after saline/OR-X pretreatment and after fentanyl. Changes in oxygen saturation were assessed as nadir (lowest value after fentanyl; **E,G,I**) and time to recover to 90% of baseline (pre-saline/OR-X; **F,H,J**) administration. Mean nadir values were assessed in saline- NLX- and NLXM-pretreated rats (Oxygen Saturation: One-way ANOVA, $F_{(2,30)} = 152.0$, $p<0.0001$; Tukey's post-hoc test, ****$p<0.0001$; Heart Rate: One-way ANOVA, $F_{(2,30)} = 38.58$, $p<0.0001$; Tukey's post-hoc test, ****$p<0.0001$; Respiratory Rate: One-way ANOVA, $F_{(2,30)} = 20.16$, $p<0.0001$; Tukey's post-hoc test, ****$p<0.0001$). Time to reach 90% baseline in saline-, NLX- and NLXM-pretreated rats. Mean time to reach 90% baseline was assessed for all parameters. Oxygen Saturation: (One-way ANOVA, $F_{(2,30)} = 81.9$, $p<0.0001$; Tukey's post-hoc test ****$p<0.0001$; Heart rate: (One-way ANOVA, $F_{(2,30)} = 44.11$, $p<0.0001$; Tukey's post-hoc test ****$p<0.0001$); Respiratory rate: (One-way ANOVA, $F_{(2,30)} = 46.74$, $p<0.0001$; Tukey's post-hoc test ****$p<0.0001$). **K.** Merged photomicrographs of a coronal brainstem section showing representative Fos- and TH- immunoreactivity in the nTS of rats that received fentanyl with or without saline or NLX/NLXM pretreatment. Scale bar = 200 µm. Fos-IR and the percentage of TH-IR neurons expressing Fos-IR was evaluated in 3 nTS sections per rat. **L.** Mean data show no significant difference in the number of Fos-IR cells between saline- and NLXM-pretreated rats. NLX-pretreated rats displayed the lowest degree of Fos-IR in the nTS. Number Fos-IR cells: One-way ANOVA, $F_{(2,18)} = 30.52$, $p<0.0001$; Tukey's post-hoc ****$p<0.0001$. **M.** Mean data of the percentage of TH-IR nTS cells expressing Fos-IR. The percentage of TH-IR cells expressing Fos-IR was similar between saline- and NLXM-pretreated rats. NLX-pretreated rats displayed the lowest percentage of Fos-IR in TH-IR nTS cells. Fos+TH/TH: (One-way ANOVA, $F_{(2,18)} = 21.33$, $p<0.0001$; Tukey's post-hoc ****$p<0.0001$; ***$p<0.001$).

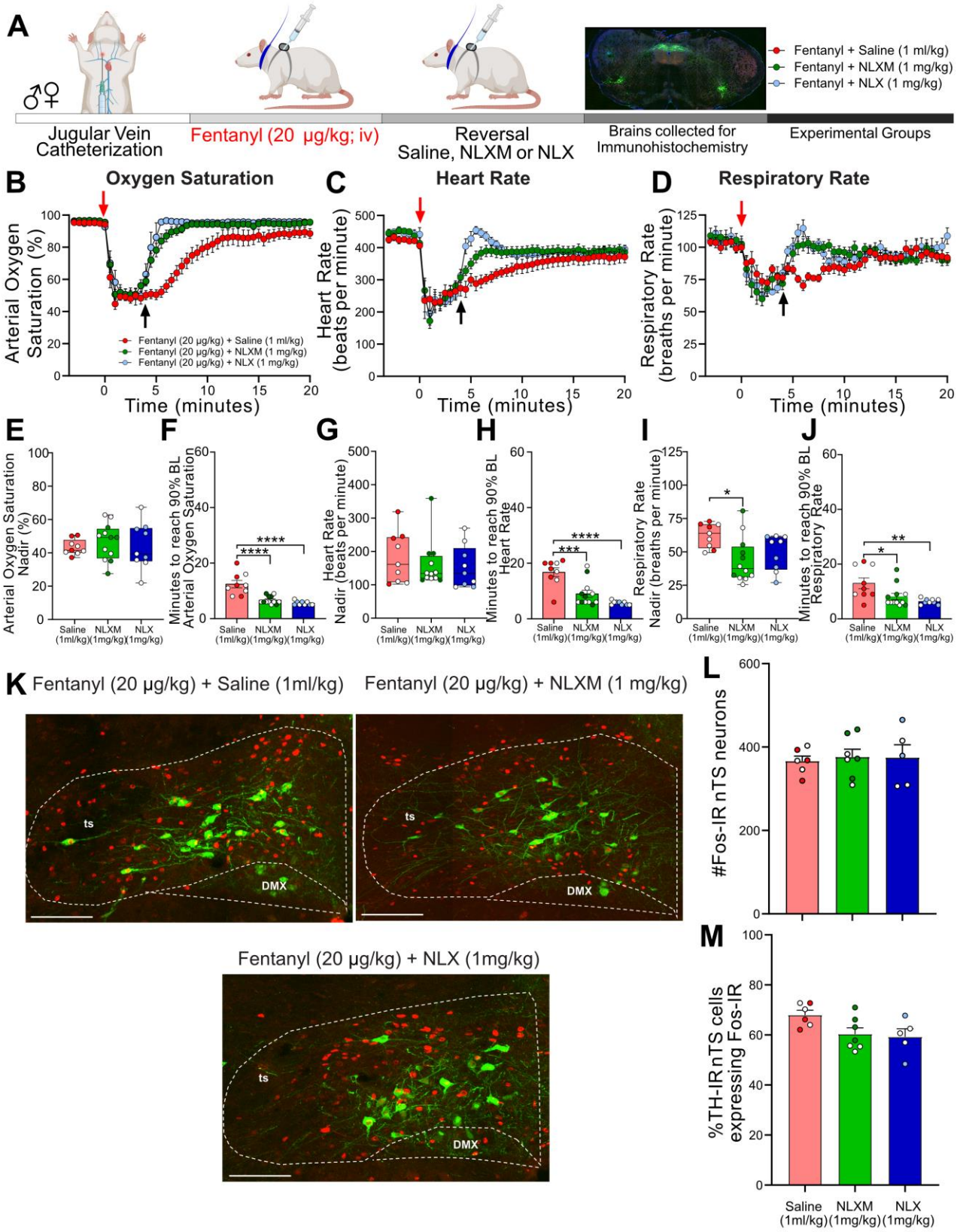
A
♂♀
Jugular Vein Catheterization
Fentanyl (20 µg/kg; iv)
Reversal Saline, NLXM or NLX
Brains collected for Immunohistochemistry
Experimental Groups
Fentanyl + Saline (1 ml/kg)
Fentanyl + NLXM (1 mg/kg)
Fentanyl + NLX (1 mg/kg)
B Oxygen Saturation
Arterial Oxygen Saturation (%)
Time (minutes)
C Heart Rate
Heart Rate (beats per minute)
D Respiratory Rate
Respiratory Rate (breaths per minute)
Fentanyl (20 µg/kg) + Saline (1 ml/kg)
Fentanyl (20 µg/kg) + NLXM (1 mg/kg)
Fentanyl (20 µg/kg) + NLX (1 mg/kg)
E Arterial Oxygen Saturation Nadir (%)
F Minutes to reach 90% BL Arterial Oxygen Saturation
G Heart Rate Nadir (beats per minute)
H Minutes to reach 90% BL Heart Rate
I Respiratory Rate Nadir (breaths per minute)
J Minutes to reach 90% BL Respiratory Rate
Saline (1ml/kg)
NLXM (1mg/kg)
NLX (1mg/kg)
K Fentanyl (20 µg/kg) + Saline (1ml/kg)
Fentanyl (20 µg/kg) + NLXM (1 mg/kg)
Fentanyl (20 µg/kg) + NLX (1mg/kg)
ts
DMX
L #Fos-IR nTS neurons
M %TH-IR nTS cells expressing Fos-IR

**Figure 3. NLXM-mediated reversal of 20 µg/kg fentanyl-induced respiratory depression is comparable to NLX. A.** Schematic showing the timeline for OIRD reversal experiments. Male and Female SD rats underwent jugular catheterization surgery. The following week, conscious rats in their home cages received intravenous fentanyl (20 µg/kg). Four minutes later, rats received intravenous administration (reversal) of either saline (1 ml/kg; n=9), NLX (1 mg/kg; n=9) or NLXM (1 mg/kg; n=12). Cardiorespiratory parameters were measured up to 60 minutes after fentanyl. At the conclusion of the experiment, brains were collected from a subset of animals in each group and processed for Fos- and TH- immunoreactivity. Time course data showing oxygen saturation (**B**), heart rate (**C**) and respiratory rate (**D**) data measurements collected in all groups before and after fentanyl and saline/antagonist administration. Changes in oxygen saturation were assessed as nadir (lowest value; **E,G,I**) and time to recover to 90% of baseline (pre-saline/OR-X; **F,H,J**) administration. Mean nadir values were assessed in saline-, NLX-, and NLXM-pretreated rats (Oxygen Saturation: One-way ANOVA, $F_{(2,27)} = 0.2916$, $p=0.7494$; Heart Rate: One-way ANOVA, $F_{(2,27)} = 0.4216$, $p=0.6602$; Respiratory Rate: One-way ANOVA, $F_{(2,27)} = 4.679$, $p=0.018$; Tukey's post-hoc test, *$p<0.05$. Mean time to reach 90% baseline was assessed for all parameters: Oxygen Saturation: One-way ANOVA, $F_{(2,27)} = 22.58$, $p<0.0001$; Tukey's post-hoc test, ****$p<0.0001$; Heart Rate: One-way ANOVA, $F_{(2,27)} = 19.39$, $p<0.0001$; Tukey's post-hoc test, ****$p<0.0001$, ***$p<0.001$; Respiratory Rate: One-way ANOVA, $F_{(2,27)} = 6.322$, $p=0.0001$;Tukey's post-hoc test, **$p<0.01$, *$p<0.05$). **K.** Merged photomicrographs of coronal brainstem sections displaying representative Fos- and TH-immunoreactivity in the nTS of rats that received fentanyl followed by saline, NLX or NLXM. Scale bar = 200 µm. **L.** Mean data of the number of Fos-IR cells evaluated in 3 nTS sections per rat. Number Fos-IR cells: One-way ANOVA, $F_{(2,15)} = 0.07269$, $p=0.9302$. **M.** Mean data of the percentage of TH-IR cells that expressing Fos-IR: One-way ANOVA, $F_{(2,15)} = 3.736$, $p=0.0482$. There were no significant differences in the number of Fos-IR cells or the percentage of TH-IR cells expressing Fos-IR between groups.

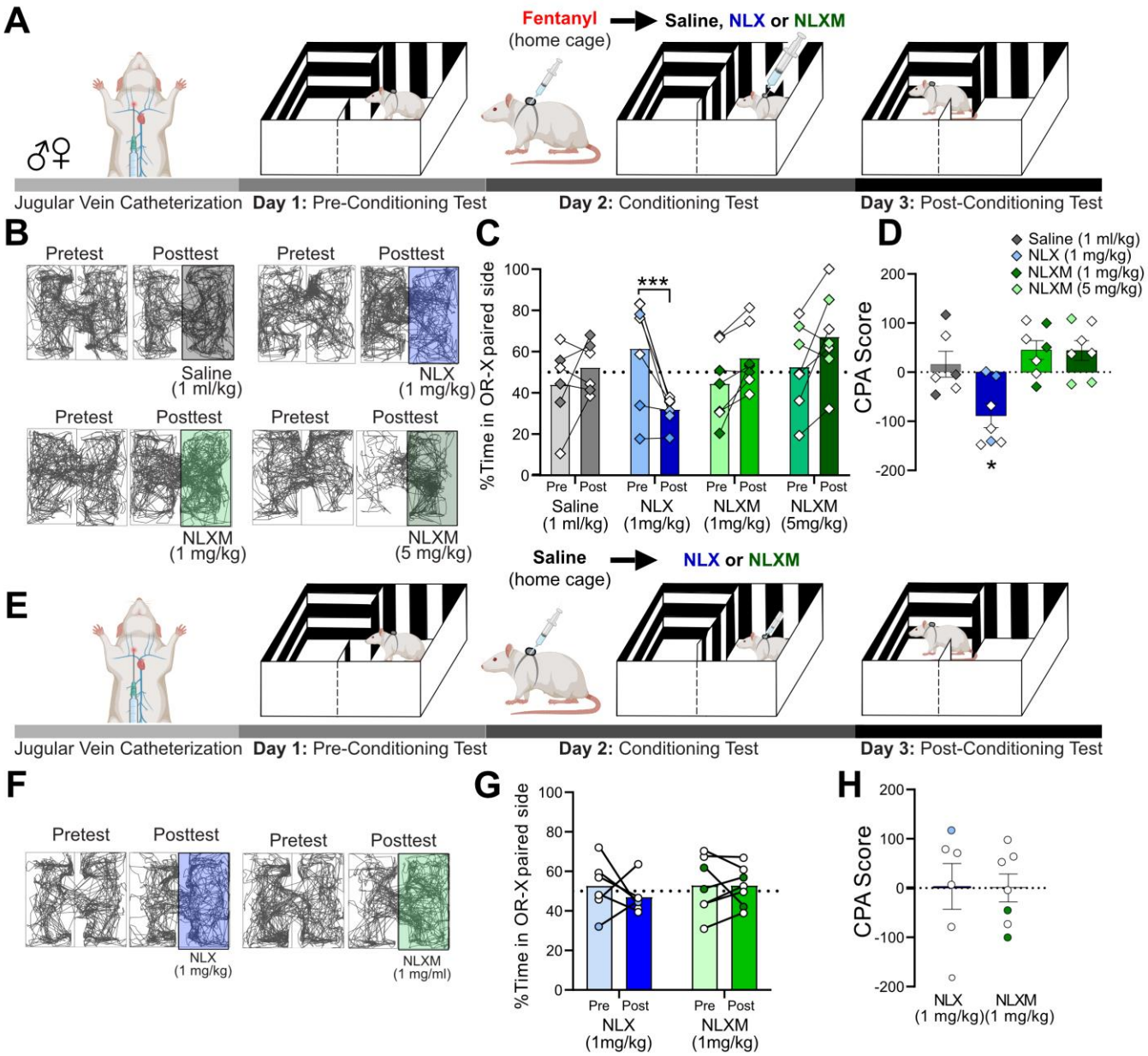
A
Fentanyl
(home cage)
Saline, NLX or NLXM
Jugular Vein Catheterization
Day 1: Pre-Conditioning Test
Day 2: Conditioning Test
Day 3: Post-Conditioning Test
B
Pretest
Posttest
Saline
(1 ml/kg)
NLX
(1 mg/kg)
NLXM
(1 mg/kg)
NLXM
(5 mg/kg)
C
% Time in OR-X paired side
***
Pre
Post
Saline
(1 ml/kg)
NLX
(1mg/kg)
NLXM
(1mg/kg)
NLXM
(5mg/kg)
D
Saline (1 ml/kg)
NLX (1 mg/kg)
NLXM (1 mg/kg)
NLXM (5 mg/kg)
CPA Score
*
Saline
(home cage)
NLX or NLXM
E
Jugular Vein Catheterization
Day 1: Pre-Conditioning Test
Day 2: Conditioning Test
Day 3: Post-Conditioning Test
F
Pretest
Posttest
NLX
(1 mg/kg)
NLXM
(1 mg/ml)
G
% Time in OR-X paired side
Pre
Post
NLX
(1mg/kg)
NLXM
(1mg/kg)
H
CPA Score
NLX
(1 mg/kg)
NLXM
(1 mg/kg)

**Figure 4: NLXM-mediated reversal of OIRD is not aversive. A**. Schematic of the Conditioned Place Aversion (CPA) experimental design for rats that received fentanyl followed by saline or an opioid receptor antagonist. Catheterized rats underwent a pre-conditioning test (Day 1). On the conditioning day (Day 2), a divider was placed in the middle of the CPA box. Rats received intravenous fentanyl (50 µg/kg) in their home cages. Four minutes later, rats were transferred to one side of the CPA box and immediately received intravenous saline (1 ml/kg, n=6), NLX (1 mg/kg, n=7), or NLXM (1 mg/kg, n=7; 5 mg/kg, n=7). During the post-conditioning test (Day 3), the divider was removed, and rats were placed in the box and allowed to explore both compartments. **B.** Track plot data showing movement in both sides of the CPA box during the Pretest (day 1) and Posttest (Day 3). For each condition, the Pre- and Posttest data is from the same animal. In these representative examples, the saline- or antagonist-paired side is shown on the right side of the box. However, the paired side was balanced between left and right sides of the box for all groups. **C.** Mean data with individual plots showing changes in the time spent in the saline- and antagonist-paired side. There was a significant decrease in the time spent in the NLX-paired side: two-way repeated measures ANOVA; drug x test interaction: $F_{(3,23)}$ = 9.994, p=0.0002; Sidak's post-hoc, ***p=0.0007. **D.** The CPA score (calculated as time spent in the saline or antagonist paired compartment during posttest minus the time spent in the same compartment during the pretest. For CPA scores, one-sample t-test from hypothetical value (no aversion). There was a significant decrease in the CPA score for 1 mg/ml NLX treated rats (t=3.642 (df=6, *p<0.05). 1 mg/ml NLXM: t=2.340, df=6 p=0.0578; 5 mg/kg NLXM: t=2.172, df=6, p=0.0729. Saline, t=0.6113 (df=5, p=0.5677). **E**. Schematic of the Conditioned Place Aversion (CPA) experimental design for saline-pretreated animals. Catheterized rats underwent a pre-conditioning test (Day 1). On the conditioning day (Day 2), a divider was placed in the middle of the CPA box. Rats received intravenous saline (1 ml/kg) in their home cages. Four minutes later, rats were transferred to one side of the CPA box and immediately received intravenous NLX (1 mg/kg, n=6) or NLXM (1 mg/kg, n=7). **F.** Track plot data showing movement in both sides of the CPA box during the Pretest (day 1) and Posttest (Day 3). The paired side was balanced between left and right sides of the box for all groups. **G.** Mean data with individual plots showing changes in the time spent on the NLX- or NLXM-paired side. There was no difference in time spent in the side paired with NLX or NLXM (two-way repeated measures ANOVA, antagonist x time, $F_{(1,11)}$ = 0.4638, p=5.099. **H.** CPA scores for NLX- and NLXM-treated animals. There was no significant difference in the CPA scores in rats that received NLX (one sample t-test, t=0.07102, df=5, p=0.9461) or NLXM (one sample t-test, t=0.005032, df=6, p=0.9961).

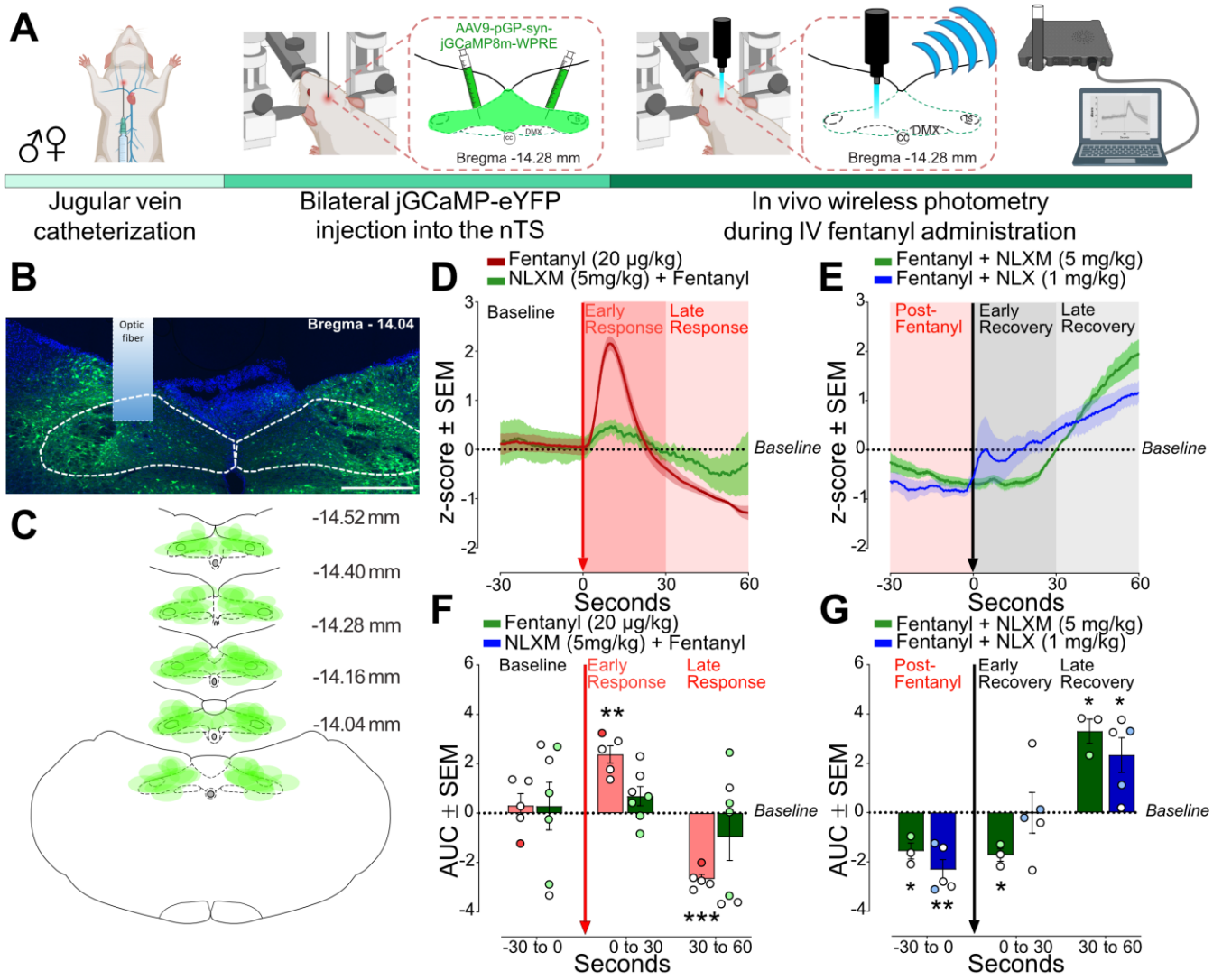
A
AAV9-pGP-syn-jGCaMP8m-WPRE
Bregma -14.28 mm
Bregma -14.28 mm
Jugular vein catheterization
Bilateral jGCaMP-eYFP injection into the nTS
In vivo wireless photometry during IV fentanyl administration
B
Optic fiber
Bregma - 14.04
C
-14.52 mm
-14.40 mm
-14.28 mm
-14.16 mm
-14.04 mm
D
Fentanyl (20 µg/kg)
NLXM (5mg/kg) + Fentanyl
Baseline
Early Response
Late Response
z-score ± SEM
Seconds
E
Fentanyl + NLXM (5 mg/kg)
Fentanyl + NLX (1 mg/kg)
Post-Fentanyl
Early Recovery
Late Recovery
F
G
AUC ± SEM
-30 to 0
0 to 30
30 to 60

**FIGURE 5: Fentanyl-induced nTS activity is mediated by peripheral MORs**.
**A.** Experimental timeline. Male and female rats underwent jugular catheterization surgery, followed by bilateral nanoinjection of jGCaMP8m into the nTS and then allowed 3-5 weeks for viral expression. On the test day, rats were anesthetized and placed in a stereotax. The nTS was exposed and a fiber was lowered into the nTS. **B.** Representative example of eYFP expression and fiber placement in the nTS. Scale bar = 200 µm. **C.** Spread of overlay of individual animal viral expression across the caudal-rostral extent of the nTS. **D.** nTS cell response (mean z-score) aligned to 20 µg/kg fentanyl administration (red arrow) at Baseline (-30-0 seconds), early response (0-30 seconds) and late response (30-60 seconds) in rats that received 20 µg/kg fentanyl only (red trace) or 5 mg/kg NLXM followed by 20 µg/kg fentanyl (green trace). **E.** Area under the curve (AUC) was calculated during baseline (-30 to 0 seconds), Early Response (0 to 30 seconds) or Late Response (30 to 60 seconds). For AUC graphs, one-sample t-test from hypothetical zero value. In rats that received fentanyl only, there was a significant increase in the AUC during the Early Phase (t=6.747, df=4, **p=0.0025) followed by a significant decrease in the Late Phase (t=14.35, df=4, ***p=0.0001). In rats that received 5 mg/kg NLXM prior to 20 µg/kg fentanyl, no differences in AUC were observed at any time point (Baseline; t=0.2916, df=6 p=0.7804; Early Phase; t=1.760, df=6 p=0.1288; 30-60 seconds; t=1.002, df=6, p=0.3548). **F.** nTS cell response (mean z-score) aligned to MOR antagonists (black arrow). Rats received iv 20 µg/kg fentanyl (Post-Fentanyl phase, -30 to 0 seconds) prior to MOR antagonist infusion of NLX (1 mg/kg, blue trace) or NLXM (5 mg/kg, green trace). Data during Early Recovery (0 to 30 seconds) and Late Recovery (30 to 60 seconds) are shown. **G.** Mean data showing AUC analyses for both groups. For all graphs, one-sample t-test from hypothetical zero value. NLXM-treated rats had a significant decrease in activity from Post-Fentanyl baseline prior to NLXM (t=4.799, df=2 * p=0.0408) and during the Early Recovery phase (t=6.683, df=2 p=0.0217), and exhibited enhanced activity above baseline during the Late Recovery phase (t=6.716, df=2, * p=0.0215). NLX-treated rats displayed a similar decrease below baseline prior to NLX. No difference from baseline was observed during the Early Recovery phase (t=0.01238, df=4 p=0.9907), and a significant increase above baseline was observed during the Late Recovery phase (t=3.318, df=4, * p=0.0294).

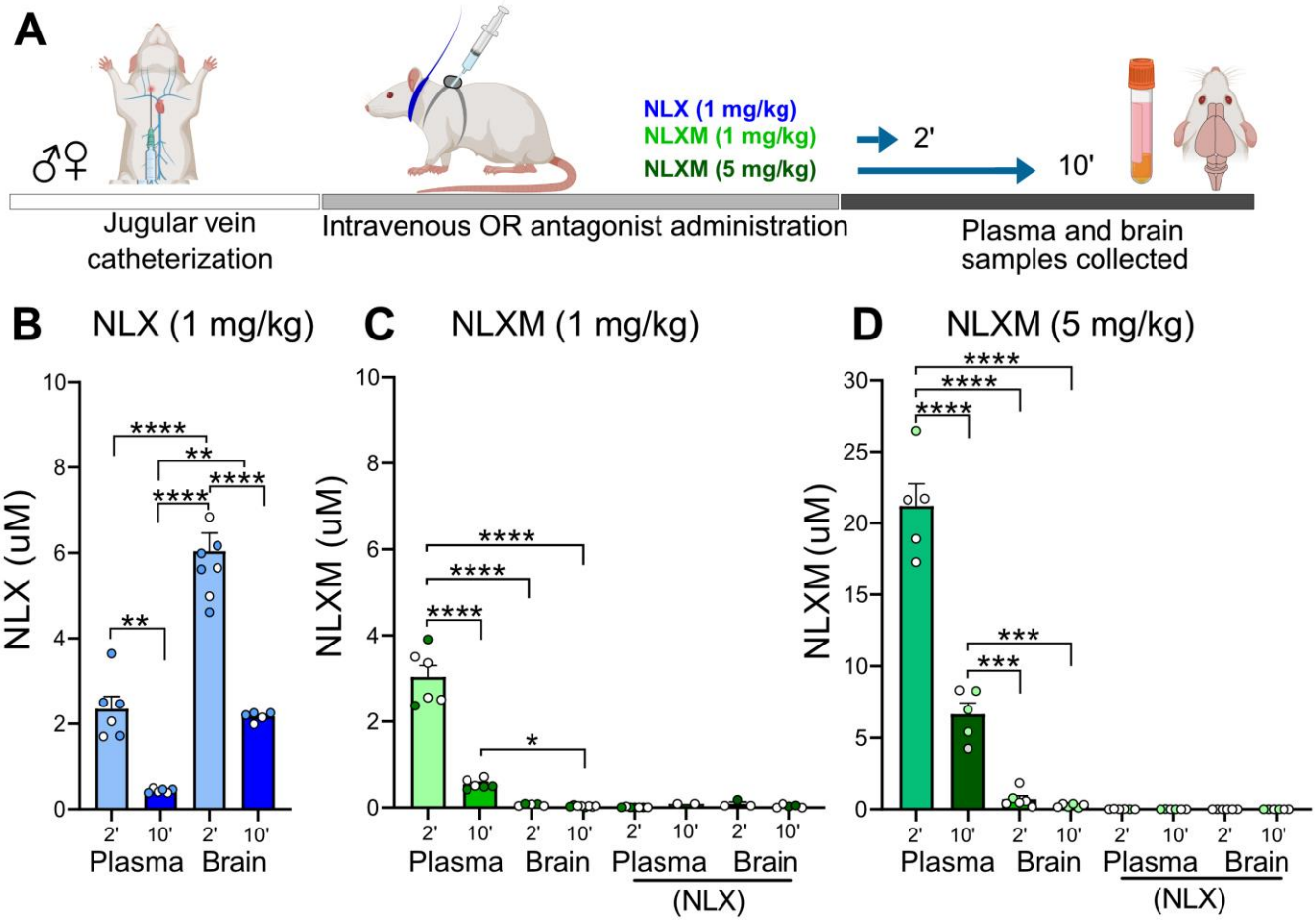


973

974

975

976

977

978

**Figure 6: NLXM does not cross the blood brain barrier**. **A**. Timeline of Biodistribution experiments. Male and female SD rats received intravenous jugular catheterization surgery. The following week, rats were anesthetized and received intravenous NLX (1 mg/kg) or NLXM (1 or 5 mg/kg). Rats were sacrificed 2- and 10- minutes after IV admin. Plasma was extracted from trunk blood and intact brains were removed and rapidly frozen with liquid nitrogen. **B**. Amount of NLX detected in plasma and brain samples at 2 and 10 minutes after intravenous NLX (1 mg/kg). One-way ANOVA, $F_{(3,21)} = 66.05$, $p < 0.0001$; Tukey's post-hoc test, **** $p<0.0001$; ** $p<0.01$. **C**. Amount of NLXM detected in plasma and brain samples at 2 and 10 minutes after intravenous NLXM (1 mg/kg). One-way ANOVA, $F_{(3,21)} = 125.6$, $p < 0.0001$; Tukey's post-hoc test, **** $p<0.0001$; * $p<0.05$. **D**. Amount of NLXM detected in plasma and brain samples at 2 and 10 minutes after intravenous NLXM (5 mg/kg). One-way ANOVA, $F_{(3,18)} = 144.0$, $p < 0.0001$; Tukey's post-hoc test, **** $p<0.0001$; *** $p<0.001$.

# Supplementary Materials for

## Peripheral opioid receptor antagonism alleviates fentanyl-induced cardiorespiratory depression and is devoid of aversive effects

[1,2,3]Brian C. Ruyle, [1,2,3]Sarah Masud, [1,2,3]Rohith Kesaraju, [1,2,3]Mubariz Tahirkheli, [1,2,3]Juhi Modh, [1,2,3]Caroline Roth, [1,2,3]Sofia Angulo-Lopera, [1,2,3]Tania Lintz, [1,2,3]Jessica A. Higginbotham, [1,2,3]Nicolas Massaly, [1,2,3,4,5]Jose A Moron*

Affiliations:

[1]Department of Anesthesiology, Washington University in St Louis; St. Louis, MO, USA

[2]Pain Center, Washington University in St Louis; St. Louis, MO, USA

[3]School of Medicine, Washington University in St. Louis; St. Louis, MO, USA

[4]Department of Neuroscience, Washington University in St. Louis; St. Louis, MO, USA

[5]Department of Psychiatry, Washington University in St. Louis; St. Louis, MO, USA

Corresponding author: jmoron-concepcion@wustl.edu

**The file includes:**

Figs. S1 to S3, Table 1-4

1036

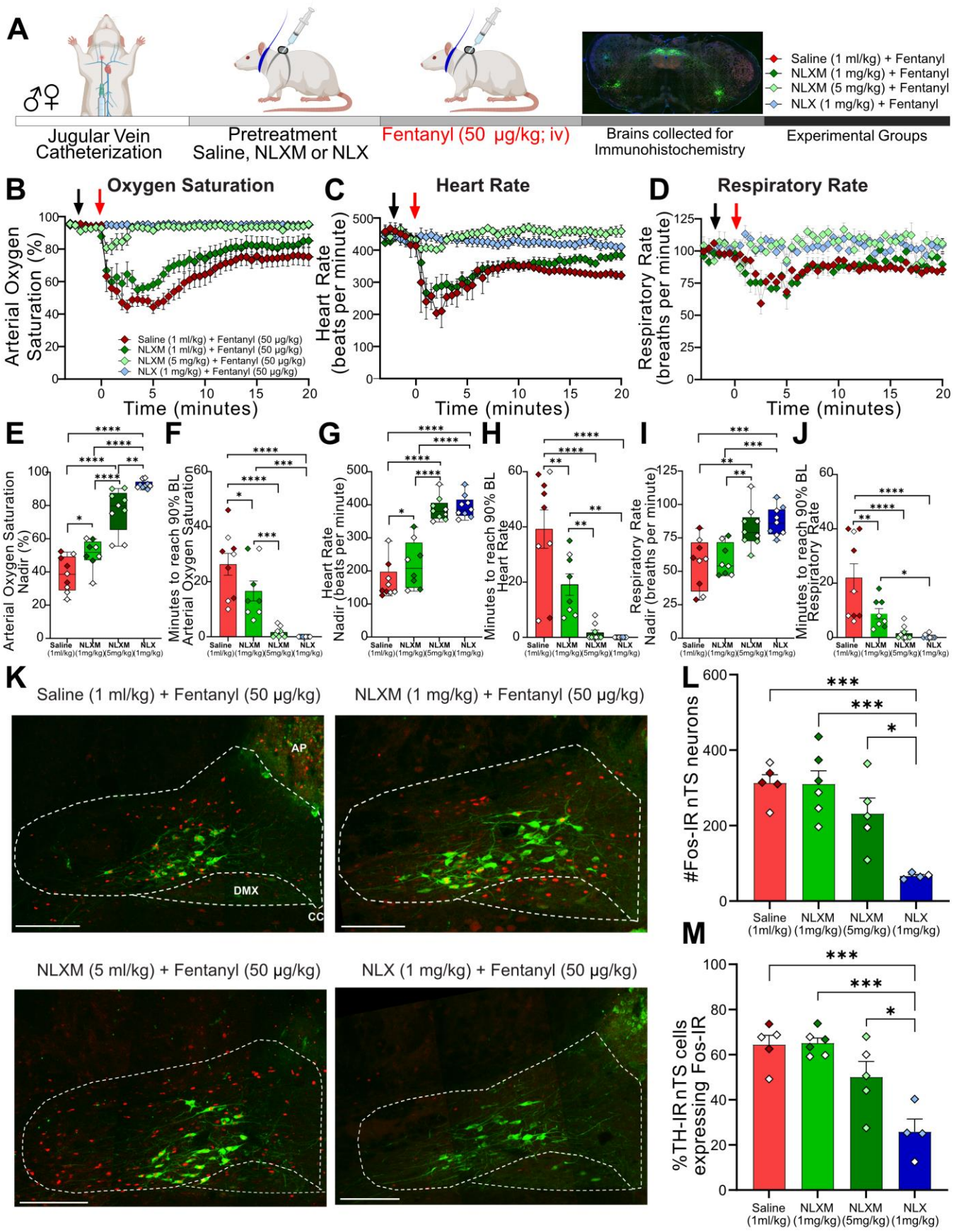
A
Jugular Vein Catheterization
Pretreatment Saline, NLXM or NLX
Fentanyl (50 µg/kg; iv)
Brains collected for Immunohistochemistry
Experimental Groups
Saline (1 ml/kg) + Fentanyl
NLXM (1 mg/kg) + Fentanyl
NLXM (5 mg/kg) + Fentanyl
NLX (1 mg/kg) + Fentanyl
B Oxygen Saturation
Arterial Oxygen Saturation (%)
Time (minutes)
Saline (1 ml/kg) + Fentanyl (50 µg/kg)
NLXM (1 ml/kg) + Fentanyl (50 µg/kg)
NLXM (5 mg/kg) + Fentanyl (50 µg/kg)
NLX (1 mg/kg) + Fentanyl (50 µg/kg)
C Heart Rate
Heart Rate (beats per minute)
D Respiratory Rate
Respiratory Rate (breaths per minute)
E Arterial Oxygen Saturation Nadir (%)
F Minutes to reach 90% BL Arterial Oxygen Saturation
G Heart Rate Nadir (beats per minute)
H Minutes to reach 90% BL Heart Rate
I Respiratory Rate Nadir (breaths per minute)
J Minutes to reach 90% BL Respiratory Rate
Saline (1ml/kg)
NLXM (1mg/kg)
NLXM (5mg/kg)
NLX (1mg/kg)
K
Saline (1 ml/kg) + Fentanyl (50 µg/kg)
NLXM (1 mg/kg) + Fentanyl (50 µg/kg)
NLXM (5 ml/kg) + Fentanyl (50 µg/kg)
NLX (1 mg/kg) + Fentanyl (50 µg/kg)
AP
DMX
CC
L #Fos-IR nTS neurons
M %TH-IR nTS cells expressing Fos-IR

**Supplemental Figure 1: Naloxone Methiodide Attenuates Fentanyl-Induced Respiratory Depression and Limits nTS Neuronal Activation. A**. Schematic showing the timeline for evaluation of reversal of OIRD. Male and Female SD rats underwent jugular catheterization surgery. On the day of the experiment, rats were administered saline (1 ml/kg), NLX (1 mg/kg) or NLXM (1 or 5 mg/kg) intravenously. Two minutes later, rats received intravenous fentanyl (50 µg/kg). Cardiorespiratory parameters were measured for up to 60 minutes after fentanyl administration. The first 20 minutes of time course data showing oxygen saturation (**B**), heart rate (**C**) and respiratory rate (**D**) measurements collected is shown for all groups. **E-J** shows the nadir of each cardiorespiratory parameter (**E,G,I**) and time to return to 90% of baseline values (pre-saline/fentanyl; **F,H,J**). For graphs displaying mean nadir values: Oxygen Saturation: One-way ANOVA, $F_{(3,31)} = 58.04$, $p < 0.0001$;Tukey's post-hoc test, **** $p<0.0001$; ** $p<0.01$; *$p<0.05$; Heart Rate: One-way ANOVA, $F_{(3,31)} = 46.34$, $p < 0.0001$; Tukey's post-hoc test, **** $p<0.0001$; *$p<0.05$; Respiratory Rate: One-way ANOVA, $F_{(3,31)} = 11.12$, $p < 0.001$;Tukey's post-hoc test, ***$p<0.001$, **$p<0.01$). For graphs displaying time to reach 90% baseline: Oxygen Saturation: (One-way ANOVA, $F_{(3,31)} = 23.00$, $p < 0.0001$; Tukey's post-hoc test ****$p<0.0001$; ***$p<0.001$; *$p<0.05$; Heart rate: (One-way ANOVA, $F_{(3,31)} = 21.13$, $p < 0.0001$; Tukey's post-hoc test ****$p<0.0001$; **$p<0.01$); Respiratory rate: (One-way ANOVA, $F_{(3,31)} = 12.79$, $p < 0.0001$; Tukey's post-hoc test, ****$p<0.0001$; **$p<0.01$; *$p<0.05$). **K**. Merged photomicrographs of a coronal brainstem section displaying Fos- and TH- immunoreactivity in the nTS from all groups. Scale bar = 200 µm. **L**. The number of Fos-IR cells was similar between saline and both NLXM treated groups. There were significantly fewer Fos cells in 1 mg/kg NLX-pretreated animals. One-way ANOVA, $F_{(3,16)} = 11.40$, $p < 0.001$; Tukey's post-hoc ***$p<0.001$; *$p<0.05$. **M** shows the percentage of TH-IR nTS neurons expressing Fos-IR. There was no significant difference between saline- and NLXM-pretreated rats. NLX-pretreated rats displayed significantly lower percentage of TH-IR nTS neurons expressing Fos-IR. One-way ANOVA, $F_{(3,16)} = 13.06$, $p=0.0001$; Tukey's post-hoc *** $p<0.001$; * $p<0.05$).

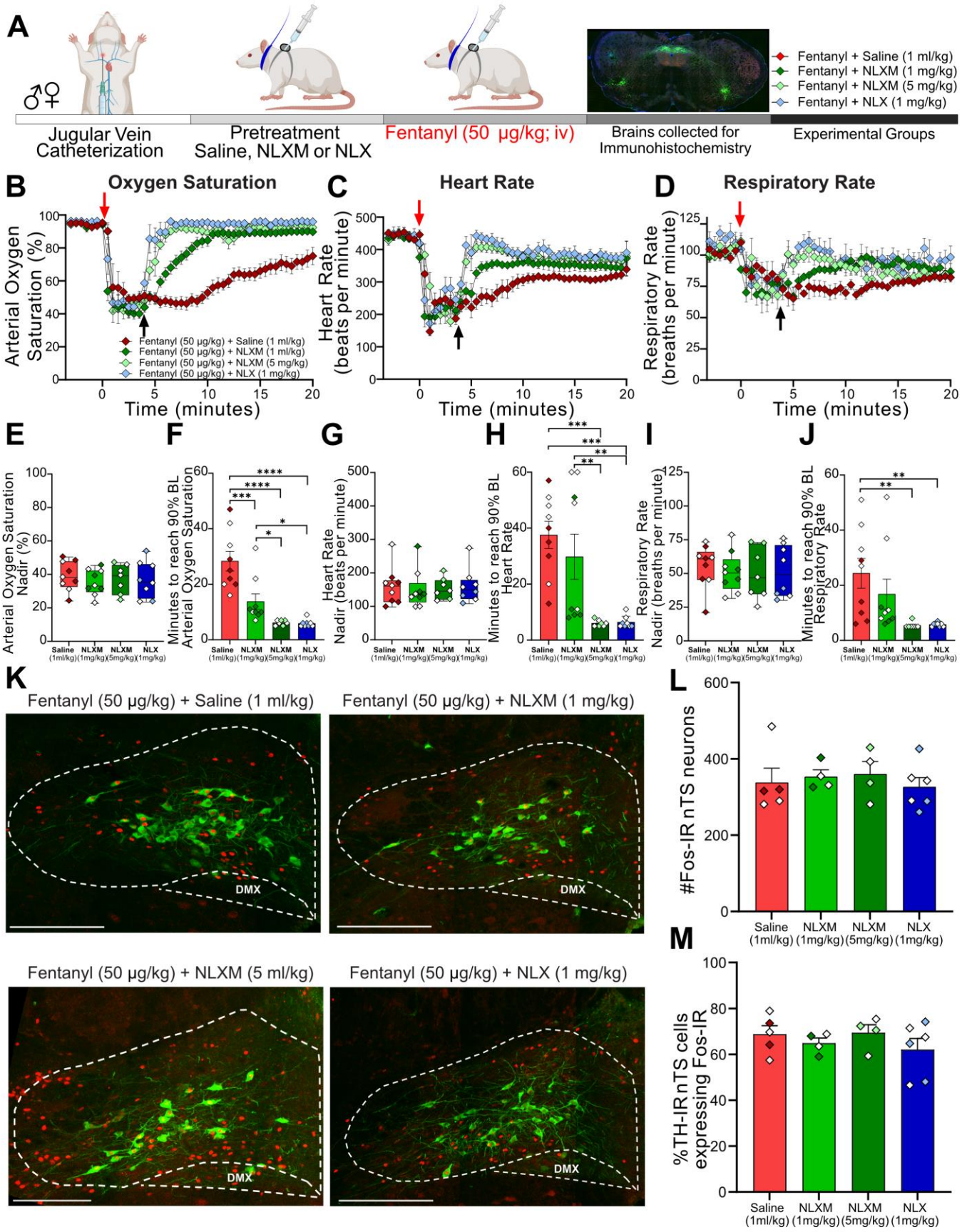
A
Jugular Vein Catheterization
Pretreatment Saline, NLXM or NLX
Fentanyl (50 µg/kg; iv)
Brains collected for Immunohistochemistry
Experimental Groups
Fentanyl + Saline (1 ml/kg)
Fentanyl + NLXM (1 mg/kg)
Fentanyl + NLXM (5 mg/kg)
Fentanyl + NLX (1 mg/kg)
B Oxygen Saturation
Arterial Oxygen Saturation (%)
Time (minutes)
C Heart Rate
Heart Rate (beats per minute)
D Respiratory Rate
Respiratory Rate (breaths per minute)
Fentanyl (50 µg/kg) + Saline (1 ml/kg)
Fentanyl (50 µg/kg) + NLXM (1 ml/kg)
Fentanyl (50 µg/kg) + NLXM (5 mg/kg)
Fentanyl (50 µg/kg) + NLX (1 mg/kg)
E Arterial Oxygen Saturation Nadir (%)
F Minutes to reach 90% BL Arterial Oxygen Saturation
G Heart Rate Nadir (beats per minute)
H Minutes to reach 90% BL Heart Rate
I Respiratory Rate Nadir (breaths per minute)
J Minutes to reach 90% BL Respiratory Rate
Saline (1ml/kg)
NLXM (1mg/kg)
NLXM (5mg/kg)
NLX (1mg/kg)
K
Fentanyl (50 µg/kg) + Saline (1 ml/kg)
Fentanyl (50 µg/kg) + NLXM (1 mg/kg)
Fentanyl (50 µg/kg) + NLXM (5 ml/kg)
Fentanyl (50 µg/kg) + NLX (1 mg/kg)
DMX
L #Fos-IR nTS neurons
M %TH-IR nTS cells expressing Fos-IR

1067

**Supplemental Figure 2: NLXM reverses respiratory depression included by a high dose of fentanyl. A**. Schematic showing the timeline for evaluation of reversal of OIRD. Male and Female SD rats underwent jugular catheterization surgery. On the day of the experiment, rats received intravenous fentanyl (50 µg/kg). Four minutes later, rats received saline (1 ml/kg), NLX (1 mg/kg) or NLXM (1 or 5 mg/kg). Cardiorespiratory parameters were collected for up to 60 minutes after saline or antagonist administration. The first 20 minutes of time course data showing oxygen saturation (**B**), heart rate (**C**) and respiratory rate (**D**) measurements collected is shown for all groups. **E-J** shows each cardiorespiratory parameter at their respective nadir (**E,G,I**) and time to recover to 90% of baseline (pre-fentanyl; **F,H,J**) administration. Mean nadir values were assessed in all groups. Oxygen Saturation: One-way ANOVA, $F_{(3,29)} = 0.2892$, $p = 0.8325$; Heart Rate: One-way ANOVA, $F_{(3,29)} = 0.09684$, $p=0.9612$; Respiratory Rate: One-way ANOVA, $F_{(3,29)} = 0.1443$, $p=0.9325$. Mean time to reach 90% baseline was assessed for all parameters. Oxygen Saturation: (One-way ANOVA, $F_{(3,29)} = 18.25$, $p <0.0001$; Tukey's post-hoc test ****$p<0.0001$; ***$p<0.001$; *$p<0.05$; Heart rate: (One-way ANOVA, $F_{(3,29)} = 9.705$, $p=0.001$; Tukey's post-hoc test ***$p<0.001$; **$p<0.01$; Respiratory rate: (One-way ANOVA, $F_{(3,29)} = 4.799$, $p <0.01$; Tukey's post-hoc test, **$p<0.01$). **K**. Merged photomicrographs of a coronal brainstem section displaying Fos- and TH- immunoreactivity in the nTS from all groups. Scale bar = 200 µm. **L**. Neuronal activation was assessed in saline- and OR-X-treated rats. Number of Fos-IR cells: One-way ANOVA, $F_{(3,15)} = 0.2689$, $p=0.8468$; **M**. Percentage of TH cells that expressing Fos-IR: (One-way ANOVA, $F_{(3,15)} = 0.7616$, $p=0.5330$.

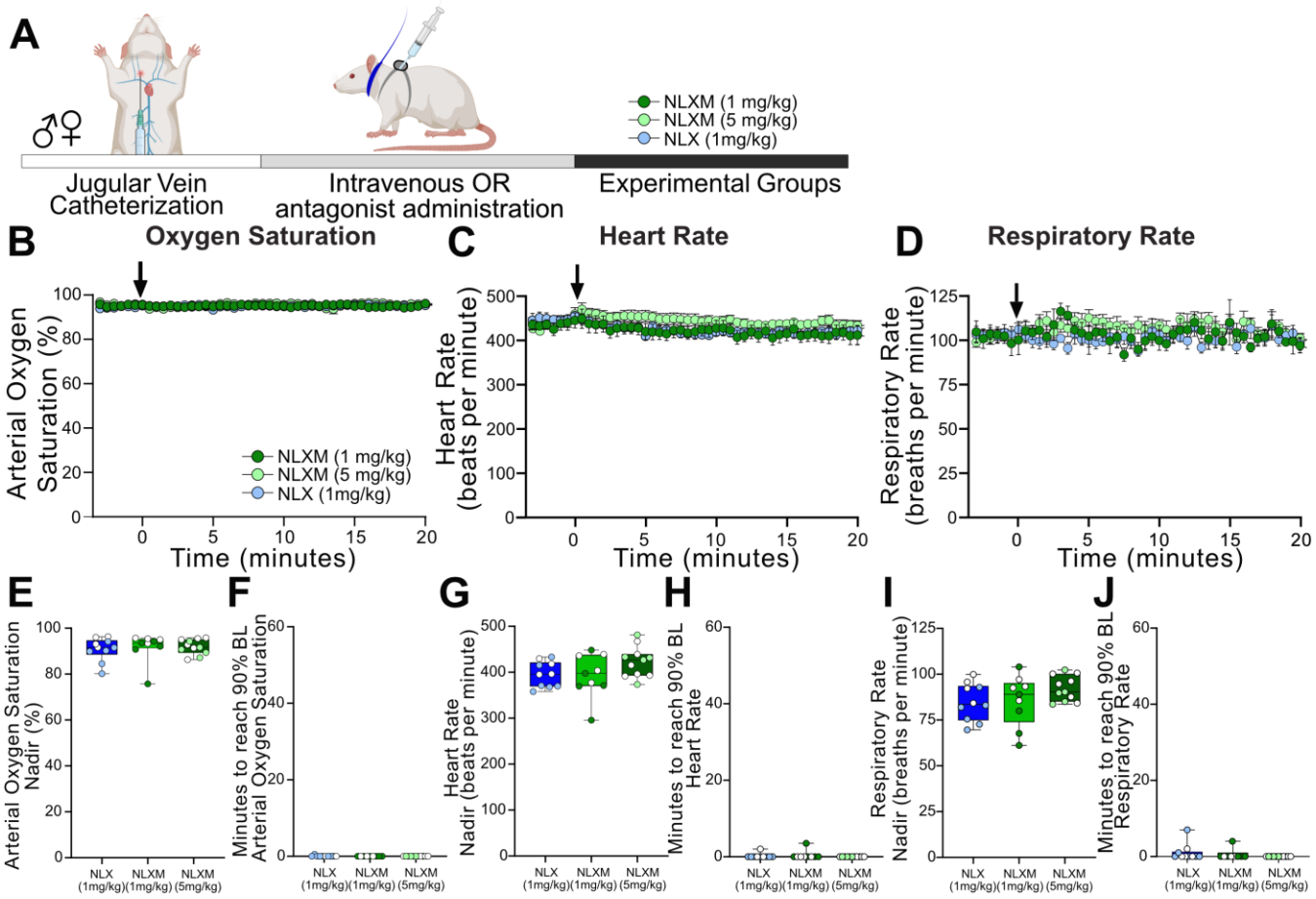
A
♂♀
NLXM (1 mg/kg)
NLXM (5 mg/kg)
NLX (1mg/kg)
Jugular Vein Catheterization
Intravenous OR antagonist administration
Experimental Groups
B
Oxygen Saturation
Arterial Oxygen Saturation (%)
Time (minutes)
C
Heart Rate
Heart Rate (beats per minute)
D
Respiratory Rate
Respiratory Rate (breaths per minute)
E
Arterial Oxygen Saturation Nadir (%)
F
Minutes to reach 90% BL Arterial Oxygen Saturation
G
Heart Rate Nadir (beats per minute)
H
Minutes to reach 90% BL Heart Rate
I
Respiratory Rate Nadir (breaths per minute)
J
Minutes to reach 90% BL Respiratory Rate
NLX (1mg/kg)
NLXM (1mg/kg)
NLXM (5mg/kg)

**Supplemental Figure 3: Opioid Receptor antagonism has no effect on baseline cardiorespiratory parameters in drug-naïve rats. A**. Schematic showing the timeline for evaluation of cardiorespiratory parameters following administration of opioid receptor antagonists in catheterized male and female SD rats. **B-D.** Rats received either intravenous (black arrow) 1 mg/kg NLX (blue symbols), 1 mg/kg NLXM (light green symbols) or 5 mg/kg NLXM (dark green symbols). Cardiorespiratory parameters were measured up to 20 minutes. The nadir and recovery of oxygen saturation (**E,F**), heart rate (**G,H**) and respiratory rate (**I,J**) was is shown for each group. For graphs displaying the nadir: Oxygen saturation: One-way ANOVA, $F_{(2,27)} = 0.1497$, $p=0.8617$; heart rate: One-way ANOVA, $F_{(2,27)} = 2.115$, $p=0.1402$; respiratory rate: One-way ANOVA, $F_{(2,27)} = 1.597$, $p=0.2211$. For graphs displaying time to recovery to 90% baseline: Oxygen saturation: One-way ANOVA, $F_{(2,27)} = 1.000$, $p=0.3811$; heart rate: One-way ANOVA, $F(2,27) = 0.7014$, $p=0.5047$; respiratory rate: One-way ANOVA, $F(2,27) = 1.216$, $p=0.3121$.

| Table 1. Baseline cardiorespiratory values in rats prior to receiving 20 µg/kg fentanyl | Figure 1 Dose Response | | Figure 2 Pretreatment | | Figure 3 Reversal | |
|---|---|---|---|---|---|---|
| | Males | Females | Males | Females | Males | Females |
| Oxygen Saturation Baseline (%) | 94 ± 0.5 | 95 ± 0.4 | 96 ± 0.4 | 96 ± 0.4 | 95 ± 0.6 | 95 ± 0.3 |
| Heart Rate Baseline (beats per minute) | 445 ± 16 | 426 ± 13 | 462 ± 12 | 439 ± 17 | 436 ± 10 | 416 ± 13 |
| Respiratory Rate Baseline (breaths per minute) | 109 ± 6 | 95 ± 3 | 108 ± 5 | 114 ± 3 | 103 ± 4 | 102 ± 4 |

**Supplemental Table 1: Baseline cardiorespiratory values in rats prior to receiving 20 µg/kg fentanyl**. Values are mean ± SE. Data from Figures 1, 2 and 3 are separated by sex. There was no significant difference in any of the measured parameters between male and female rats. Oxygen saturation: one-way ANOVA, $F_{(5, 27)} = 0.6787$, $p = 0.6424$; heart rate: one-way ANOVA, $F_{(5, 27)} = 1.078$, $p=0.3944$; respiratory rate: one-way ANOVA, $F_{(5, 27)} = 1.527$, $p=0.2147$.

| Table 2. Baseline cardiorespiratory values in male and female rats prior to 50 µg/kg fentanyl | Figure 1 Dose Response | | Figure S1 Pretreatment | | Figure S2 Reversal | |
|---|---|---|---|---|---|---|
| | Males | Females | Males | Females | Males | Females |
| Oxygen Saturation Baseline (%) | 94 ± 1 | 95 ± 1 | 94 ± 1 | 96 ± 1 | 94 ± 1 | 95.2 ± 1.1 |
| Heart Rate Baseline (beats per minute) | 408 ± 10 | 485 ± 13 † | 450 ± 21 | 434 ± 14 | 421 ± 17 | 451 ± 33 |
| Respiratory Rate Baseline (breaths per minute) | 95 ± 2 | 110 ± 4 | 101 ± 5 | 98 ± 4 | 100 ± 1 | 105 ± 8 |

**Supplemental Table 2: Baseline cardiorespiratory values in male and female rats prior to receiving 50 µg/kg fentanyl**. Values are mean ± SE. Data from Figures 1, S1 and S2 are separated by sex. Female rats in Figure 1 had a significantly higher heart rate at baseline compared male rats in Figure 1. Oxygen saturation: one-way ANOVA, $F_{(5, 25)} = 1.161$, $p=0.3558$; heart rate: one-way ANOVA, $F_{(5, 25)} = 3.774$, $p=0.0110$, Tukey's post-hoc test † $p<0.05$ Figure 1 males vs Figure 1 females; respiratory rate: one-way ANOVA, $F_{(5, 25)} = 1.728$, $p=0.1649$.

| Table 3. Nadir and recovery values in male and female rats that received 20 µg/kg fentanyl | Figure 1 Dose Response | | Figure 2 Pretreatment | | Figure 3 Reversal | |
|---|---|---|---|---|---|---|
| | Males | Females | Males | Females | Males | Females |
| Oxygen Saturation Nadir (%) | 50 ± 4 | 50 ± 4 | 42 ± 6 | 38 ± 1 | 53 ± 6 | 45 ± 2 |
| Heart Rate Nadir (beats per minute) | 182 ± 26 | 144 ± 10 | 253 ± 32 | 177 ± 55 | 226 ± 45 | 146 ± 20 |
| Respiratory Rate Nadir (breaths per minute) | 59 ± 3 | 49 ± 4 | 67 ± 4 | 45 ± 12 | 66 ± 5 | 60 ± 4 |
| Oxygen Saturation Recovery (minutes) | 11 ± 1 | 10 ± 1 | 12 ± 2 | 14 ± 2 | 14 ± 3 | 11 ± 1 |
| Heart Rate Recovery (minutes) | 15 ± 13 | 16 ± 1 | 15 ± 3 | 13 ± 5 | 15 ± 3 | 18 ± 1 |
| Respiratory Rate Recovery (minutes) | 12 ± 2 | 14 ± 1 | 10 ± 1 | 17 ± 4 | 11 ± 1 | 15 ± 3 |

**Supplemental Table 3: Nadir and recovery values in male and female rats that received 20 µg/kg fentanyl**. Values are mean ± SE. Data from Figures 1, 2 and 3 are separated by sex. For nadir data: oxygen saturation: one-way ANOVA, $F_{(5, 27)} = 1.229$, $p = 0.3230$; heart rate: one-way ANOVA, $F_{(5, 27)} = 1.844$, $p=0.1379$; respiratory rate: one-way ANOVA, $F_{(5, 27)} = 2.669$, $p=0.0438$. Despite the significant interaction for respiratory rate, no post hoc differences were detected. Sex differences in recovery times were also evaluated. oxygen saturation: one-way ANOVA, $F_{(5, 27)} = 0.7021$, $p = 0.6267$; heart rate: one-way ANOVA, $F_{(5, 27)} = 0.4536$, $p=0.8069$; respiratory rate: one-way ANOVA, $F_{(5, 27)} = 1.100$, $p=0.3832$.

| Table 4. Nadir values in male and female rats that received 50 µg/kg fentanyl | Figure 1 Dose Response | | Figure S1 Pretreatment | | Figure S2 Reversal | |
|---|---|---|---|---|---|---|
| | Males | Females | Males | Females | Males | Females |
| Oxygen Saturation Nadir (%) | 30 ± 3 | 37 ± 2 | 41 ± 4 | 35 ± 6 | 40 ± 5 | 38 ± 4 |
| Heart Rate Nadir (beats per minute) | 181 ± 16 | 145 ± 20 | 159 ± 17 | 179 ± 37 | 135 ± 17 | 188 ± 33 |
| Respiratory Rate Nadir (breaths per minute) | 48 ± 6 | 41 ± 5 | 56 ± 10 | 55 ± 9 | 50 ± 8 | 61 ± 6 |
| Oxygen Saturation Recovery (minutes) | 31± 6 | 28 ± 7 | 30 ± 5 | 22 ± 6 | 29 ± 5 | 28 ± 6 |
| Heart Rate Recovery (minutes) | 23 ± 5 | 48 ± 1 | 43 ± 9 | 33 ± 5 | 35 ± 7 | 41 ± 1 |
| Respiratory Rate Recovery (minutes) | 16 ± 3 | 43 ± 1 †# | 26 ± 7 | 18 ± 4 | 13 ± 4 | 38 ± 3 |

**Supplemental Table 4: Nadir and recovery values in male and female rats that received 50 µg/kg fentanyl**. Values are mean ± SE. Data from Figures 1, 2 and 3 are separated by sex. For nadir data: oxygen saturation: one-way ANOVA, $F_{(5, 25)} = 1.384$, $p = 0.2639$; heart rate: one-way ANOVA, $F_{(5, 25)} = 0.8879$, $p=0.5039$; respiratory rate: one-way ANOVA, $F_{(5, 25)} = 1.154$, $p=0.3591$. Sex differences in recovery times were also evaluated. oxygen saturation: one-way ANOVA, $F_{(5, 25)} = 0.2277$, $p = 0.9469$; heart rate: one-way ANOVA, $F_{(5, 25)} = 1.591$, $p=0.1992$; respiratory rate: one-way ANOVA, $F_{(5, 25)} = 4.258$, $p=0.0061$. Tukey's post-hoc test † $p<0.05$ Figure 1 males vs Figure 1 females, # $p<0.05$ Figure 1 females vs Figure S2 males.